



COLORADO
Department of Transportation

Applied Research and Innovation Branch

DEVELOPMENT OF COST-EFFECTIVE ULTRA-HIGH PERFORMANCE CONCRETE (UHPC) FOR COLORADO'S SUSTAINABLE INFRASTRUCTURE

Yail Jimmy Kim, Ph.D., P.Eng., F.ACI
University of Colorado Denver

Report No. CDOT-2018-15
May 2018

The contents of this report reflect the views of the author(s), who is(are) responsible for the facts and accuracy of the data presented herein. The contents do not necessarily reflect the official views of the Colorado Department of Transportation or the Federal Highway Administration. This report does not constitute a standard, specification, or regulation.

Technical Report Documentation Page

1. Report No. CDOT-2018-15		2. Government Accession No.		3. Recipient's Catalog No.	
4. Title and Subtitle Development of Cost-Effective Ultra-High Performance Concrete (UHPC) for Colorado's Sustainable Infrastructure				5. Report Date May 18, 2018	
				6. Performing Organization Code	
7. Author(s) Yail Jimmy Kim				8. Performing Organization Report No. CDOT-2018-15	
9. Performing Organization Name and Address University of Colorado Denver 1200 Larimer St., Denver, CO 80217				10. Work Unit No. (TRAIS)	
				11. Contract or Grant No. 215-04	
12. Sponsoring Agency Name and Address Colorado Department of Transportation - Research 4201 E. Arkansas Ave. Denver, CO 80222				13. Type of Report and Period Covered Final	
				14. Sponsoring Agency Code	
15. Supplementary Notes Prepared in cooperation with the US Department of Transportation, Federal Highway Administration					
16. Abstract This report presents the development of ultra-high performance concrete (UHPC) using locally available materials that reduce construction costs compared with commercial products. With the aim of achieving a specified compressive strength of 20 ksi, a UHPC mixture is formulated. The implications of various constituent types are examined with an emphasis on silica compounds (silica fume, silica powder, silica sand, finer silica sand, pyrogenic silica, and precipitated silica), including steel and polypropylene fibers. Bond tests are conducted to evaluate the development length of the UHPC. Cost analysis shows that the prototype UHPC is up to 74% less expensive than commercial products. Implementation A step-by-step procedure is recommended in tandem with quality assurance and quality control for CDOT to implement the UHPC technology in bridge construction.					
17. Keywords cost-effective; development; practice recommendations; silica; ultra-high-performance concrete (UHPC)			18. Distribution Statement This document is available on CDOT's website http://www.coloradodot.info/programs/research/pdfs		
19. Security Classif. (of this report) Unclassified		20. Security Classif. (of this page) Unclassified		21. No. of Pages	22. Price

ACKNOWLEDGMENTS

The research team would like to acknowledge the valuable guidance and thought-provoking comments provided by the study panel members: Mike Mohseni (now with the City of Aurora), Andrew Pott (Bridge Design and Management Branch), Eric Prieve (Materials and Geotechnical Branch), and Matt Greer (Federal Highway Administration). The research team is also grateful to the member of the Applied Research and Innovation Branch (Aziz Khan, Roberto DeDios, and Numan Mizyed) for their comprehensive support and administrative assistance.

Executive Summary

This report presents the development of ultra-high performance concrete (UHPC) using locally available materials, that reduce construction costs compared with commercial products. With the aim of achieving a specified compressive strength of 20 ksi, a UHPC mixture is formulated. The research program consists of three phases: i) suitable constituents are identified based on the reproduction tests of nine existing UHPC mixtures selected from literature, ii) a prototype mixture design is developed, and iii) the performance of the prototype UHPC is assessed through an experimental parametric study. The implications of various constituent types are examined with an emphasis on silica compounds (silica fume, silica powder, silica sand, finer silica sand, pyrogenic silica, and precipitated silica), including steel and polypropylene fibers. The distribution of granular particles is characterized by digital microscopy alongside an image processing technique. Benchmark tests employing the nine mixtures clarify that silica sand and finer silica sand perform better than silica powder from strength perspectives, and the inclusion of steel fibers rather than polypropylene fibers is recommendable. High-range water reducers (HRWR) or plasticizers marginally affect the strength of the UHPC. Although heat curing increases concrete strength, the prototype UHPC is designed with conventional moisture curing because of practicality in the field. The workability of the UHPC at a water-cement ratio of $w/c = 0.22$ is satisfactory with a slump of 8 in. The steel fibers increase the flexural capacity of the UHPC more than 60% relative to the UHPC mixed without fibers, and result in a gradual failure mode. The bulk density of silica fume influences the strength gain of the UHPC at 7 days, beyond which its effect becomes insignificant. The use of pyrogenic silica and precipitated silica is not suggested. The applicability of the modulus of rupture equations specified in published specifications and codes is assessed, and new equations are proposed for the developed UHPC mixture using randomly generated statistical data. According to bond tests, the development length of the UHPC is shorter than the requirement of the American Association of State Highway Transportation Officials (AASHTO) Load and Resistance Factor Design (LRFD) Bridge Design Specifications. Cost analysis shows that the prototype UHPC is up to 74% less expensive than commercial products. A step-by-step procedure is recommended in tandem with quality assurance and quality control for CDOT to implement the UHPC technology in bridge construction.

UHPC mixture design

<i>w/c</i>	Water (lb/yd ³)	Cement (lb/yd ³)	Silica fume (lb/yd ³)	Finer silica sand (lb/yd ³)	Silica sand (lb/yd ³)	HRWR (oz/yd ³)
0.22	334	1,517	280	512	1,582	557

Steel fibers can be added (303 lb/yd³)

Keywords: cost-effective; development; practice recommendations; silica; ultra-high-performance concrete (UHPC)

List of Tables

Table 1. Properties of constituents from manufacturers.....	3
Table 2. Properties of pyrogenic/precipitated silica from manufacturers.....	4
Table 3. Overview of experimental program.....	6
Table 4. Benchmark UHPC mixture designs.....	8
Table 5. Finalized UHPC mixture design.....	14
Table 6. Mixture designs for slump tests.....	16
Table 7. Mixture designs with various pyrogenic/precipitated silica admixtures.....	19
Table 8. Mixture designs with/without steel fiber.....	20

List of Figures

Fig. 1. Selected materials.....	4
Fig. 2. Mixing procedure.....	6
Fig. 3. Test details.....	10
Fig. 4. Image processing for particle distribution.....	11
Fig. 5. Particle size distribution.....	12
Fig. 6. Reproduction of existing design mixtures.....	13
Fig. 7. Experimental parametric study.....	17
Fig. 8. Effect of pyrogenic/precipitated silica.....	18
Fig. 9. Assessment of modulus of rupture expressions.....	20
Fig. 10. Load-displacement of UHPC prisms.....	21
Fig. 11. Crack development of specimen with steel fibers.....	22
Fig. 12. Modulus of rupture expression with Monte Carlo simulation.....	24
Fig. 13. Bond test results.....	26
Fig. 14. Cost analysis.....	27
Fig. 15. Control charts for quality control.....	28

Table of Contents

Acknowledgments.....	i
Executive Summary.....	ii
List of Tables.....	iv
List of Figures.....	v
Table of Contents.....	vi
1. Introduction.....	1
1.1. Background and Problem Statement.....	1
1.2. Objectives of Research.....	1
1.3. Organization of Report.....	2
2. Test Program.....	3
2.1. Materials.....	3
2.1.1. Cement.....	3
2.1.2. Silica sand.....	4
2.1.3. Silica fume.....	4
2.1.4. Pyrogenic silica.....	5
2.1.5. Precipitated silica.....	5
2.1.6. High-range water reducer.....	5
2.1.7. Steel fiber.....	5
2.1.8. Polypropylene fiber.....	6
2.2. Mixing procedure.....	6
2.3. Specimen Preparation.....	7
2.4. Curing condition.....	8
2.5. Mechanical testing.....	9
3. Experimental Results.....	11
3.1. Distribution of particle size.....	11
3.2. Strength of benchmark UHPC mixtures.....	13
3.3. Determination of UHPC mixture proportion.....	14
3.3.1. Cement.....	14
3.3.2. Water.....	15

3.3.3. Silica fume.....	15
3.3.4. Finer silica sand.....	15
3.3.5. Silica sand.....	15
3.3.6. High-range water reducer.....	16
3.3.7. Steel fiber.....	16
3.4. Parametric investigations.....	16
3.4.1. Workability.....	16
3.4.2. Silica fume type.....	17
3.4.3. Pyrogenic/precipitated silica.....	19
3.4.4. Strength with steel fibers.....	21
3.5. Crack development.....	23
3.6. Modulus of rupture.....	23
3.7. Bond and development length.....	25
4. Cost Analysis.....	27
5. Implementation Plan and Quality Assurance/Control.....	28
6. Summary and Conclusions.....	30
7. References.....	32
Appendix A. Test Data.....	37
Appendix B. State of the Art of UHPC.....	44

1. Introduction

1.1. Background and Problem Statement

Sustainable highway infrastructure is one of the primary interests across the nation. Among many promising materials, ultra-high performance concrete (UHPC) has been attracting state and federal agencies because of its superior mechanical properties and durability compared with ordinary concrete (Graybeal 2009; Russell and Graybeal 2013). UHPC is a cementitious composite material consisting of portland cement, water, a high-range water reducer or superplasticizer, fine aggregate, and other admixtures. Supplementary fibers may be added to enhance the tensile resistance. The compressive strength of UHPC is typically over 130 MPa (18 ksi) with a tensile strength of 12 MPa (1,740 psi) (Resplendino 2008). On many occasions, the water-cement ratio of UHPC is lower than $w/c = 0.25$ to accomplish such a high strength. From a durability standpoint, the porosity of densely-mixed UHPC plays an important role in impeding the flow of water; hence, environment-assisted damage is precluded (FHWA 2011). A number of highway bridges have been constructed using UHPC around the world (Blais and Couture 1999; Russell and Graybeal 2013), including the Jakway Park Bridge in Iowa (Rouse et al. 2011). A noticeable drawback of UHPC can be found in high material costs. Although the costs may be counterbalanced by its outstanding performance at minimal maintenance effort (Semioli 2001), end-user sectors are often reluctant to adopt this expensive material for construction projects. To facilitate the use of UHPC in bridge applications, material costs should be reduced by developing a mixture with locally available constituents. Furthermore, it is hard to fully implement the UHPC technologies in the State of Colorado owing to a lack of codes, standards, and practice manuals. The present research aims to develop cost-effective UHPC for the benefit of bridge construction in Colorado without paying extra dollars required to purchase commercial products. The emphasis of this technical report is placed on experimental investigations, quality assurance and quality control, and practice recommendations for site implementation. Appendices are provided to detail test data and to inform CDOT of the state of the art of UHPC technologies.

1.2. Objectives of Research

The objective of the research is to develop cost-effective UHPC mixtures ($f'_c = 20$ ksi) using locally available materials in Colorado. In so doing, construction costs will be reduced while maintaining engineering properties comparable to commercial UHPC products. The research

program is comprised of experimental investigations, cost analysis, and recommendations for implementation along with quality assurance and quality control.

1.3. Organization of Report

Chapter 1 discusses an overview of the research background to justify the need for developing a cost-effective UHPC mixture, which will benefit the economy and infrastructure of Colorado. Chapter 2 details an experimental program with a focus on material constituents, mixing procedure, specimen preparation, curing conditions, bond, and mechanical testing. Chapter 3 provides the test results of various concrete mixtures, including material characterizations and compressive/flexural load-carrying capacities as well as the bond between the UHPC and reinforcement. Chapter 4 elaborates on the costs of each constituent and the total costs of the developed UHPC are compared with those of commercial products. Chapter 5 deals with an implementation plan and quality assurance/control. Chapter 6 summarizes the research program and draws technical conclusions. Appendices A and B present test data and a state-of-the-art review of UHPC, respectively.

2. Test Program

An experimental program is conducted to develop a cost-effective UHPC with locally available materials at a target compressive strength of $f'_c = 20$ ksi. This section delineates constituents, mixing, specimens, curing, and mechanical testing.

2.1. Materials

The descriptions of constituent materials to mix UHPC are provided, as follows.

2.1.1. Cement

High-early strength portland cement (Type III of ASTM C150, ASTM 2017) was the primary binder of a UHPC mixture. Although the composition of Type III is similar to that of Type I (ordinary cement), the former's finer grains accelerate a strength gain rate (Mehta and Monteiro 2014). The use of Type III is thus beneficial, particularly for accelerated bridge construction such as closure joints between adjacent precast girders. It is also advantageous when UHPC is cast at low temperatures (construction in winter) since Type III generates curing heat, which facilitates the hydration of the concrete in such an environment.

Table 1. Properties of constituents from manufacturers

	Properties	
Silica powder	SiO ₂ = 99.8%; SG = 2.65; pH = 7.2	
Silica sand	SiO ₂ = 90.3%; SG = 2.62; pH = 7.0	
Finer silica sand	SiO ₂ = 99.8%; SG = 2.65; pH = 7.2	
Silica fume	Type A	SiO ₂ ≥ 85%; SG = 2.26
	Type B	SiO ₂ (amorphous) ≥ 85%; SiO ₂ (crystalline) ≤ 0.5%; BD = 30 lb/ft ³ ; pH = 6
	Type C	SiO ₂ ≥ 85%; BD = 38 lb/ft ³
	Type D	SiO ₂ ≥ 98%; pH = 6.7; BD = 19 lb/ft ³
Steel fiber	$f_u = 313$ ksi; $E_s = 30,500$ ksi; SG = 7.85	
Polypropylene fiber	$f_u = 96$ ksi; $l = 0.75$ in.; SG = 0.91	

SG = specific gravity; BD = bulk density; pH = potential of hydrogen; f_u = tensile strength; E_s = elastic modulus; l = fiber length

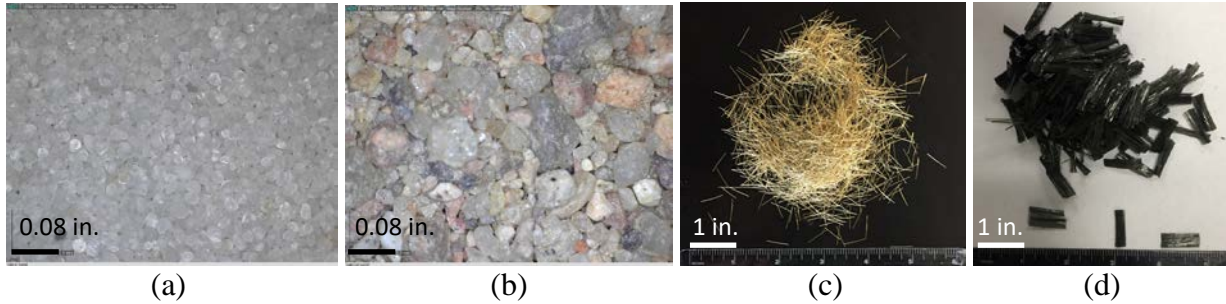


Fig. 1. Selected materials: (a) silica sand; (b) natural sand; (c) steel fiber; (d) polypropylene fiber

2.1.2. Silica sand

Silica sand is quartz granules and includes more SiO_2 compared with natural sand. Two types of silica sand were employed: ordinary and finer classes. The ordinary silica sand possesses an SiO_2 amount of 90.3%, while the finer one involves 99.8%, as shown in Table 1. The effective size of the ordinary and finer silica sands (determined from sieve analysis) is 0.016 to 0.02 in. and 0.006 to 0.012 in., respectively, according to the manufacturers. A silica powder product (Table 1) was also included in one of the mixture designs studied (discussion follows). Figures 1(a) and (b) show the configurations of silica sand and natural sand, respectively. The shape of silica sand particles is spherical at a relatively constant size, whereas that of natural sand is irregular. As such, the former is expected to have better rheological characteristics in a concrete mixture than the latter.

Table 2. Properties of pyrogenic/precipitated silica from manufacturers

Taxonomy	Pyrogenic silica	Precipitated silica
Specific surface area	976 ft^2/kip	928 ft^2/kip
Average primary particle size	5×10^{-7} in.	5×10^{-3} in.
Tampered density	3×10^{-3} lb/oz	17×10^{-3} lb/oz
pH	4.7	6.5
SiO_2 content	99.8 wt/%	97 wt/%

pH = potential of hydrogen

2.1.3. Silica fume

Silica fume, a by-product of silicon and ferrosilicon alloys, is often called microsilica owing to its particle size being much smaller than cement particles (to be detailed in a subsequent section).

The particles are typically obtained from SiO vapors after oxidization and condensation processes. Silica fume that fills the micro-void of cement reduces the porosity and permeability of the concrete, which is beneficial from strength and durability perspectives, when a reasonable amount (more than 10% of the cement mass) is mixed. To facilitate the use of silica fume in a concrete mixture, high-range water reducers are required because the fine particle size of silica fume consumes curing water that is necessary for the hydration of the cement to occur. Four types of silica fume products were exploited, as enumerated in Table 1, including variable SiO₂ amounts and bulk densities. ASTM C1240 (ASTM 2015a) requires a minimum amount of SiO₂ be 85%.

2.1.4. Pyrogenic silica

This nano-scale silica product, manufactured by a flame of hydrogen alongside chlorosilane, has a SiO₂ purity of 99.8% and a specific surface area of 976 ft²/kip (Table 2). Pyrogenic silica is chemically inert and enhances the flowability and abrasion of a mixture system.

2.1.5. Precipitated silica

Obtained by precipitation resulting from chemical reactions of alkali silicate (Garrett 1993), precipitated silica possesses a high SiO₂ content of 97%. Despite a specific surface area similar to the area of the pyrogenic silica, the particle size of the precipitated silica is much larger (Table 2).

2.1.6. High-range water reducer

Due to the aforementioned fine cementitious materials that decrease workability, the use of a high-range water reducer (HRWR) is indispensable for UHPC mixtures. A polycarboxylate-based HRWR, consisting of carboxylate and oligo ethylene oxide, was employed to generate linear polymers that enclose and distribute cement particles (electrostatic repulsion, Habbaba et al. 2013) without changing a mix composition. The HRWR inhibits water-bleeding, which is advantageous in attaining quality concrete.

2.1.7. Steel fiber

Round steel microfibers were used to improve the toughness and crack resistance (initiation and growth) of UHPC, including plastic shrinkage cracking. The length and diameter of the fibers are 0.5 in. and 0.008 in., respectively (Fig. 1(c)): the aspect ratio is 65, which is typical in steel fibers (30 to 150, Mehta and Monteiro 2014). Table 1 details the mechanical properties of the fibers.

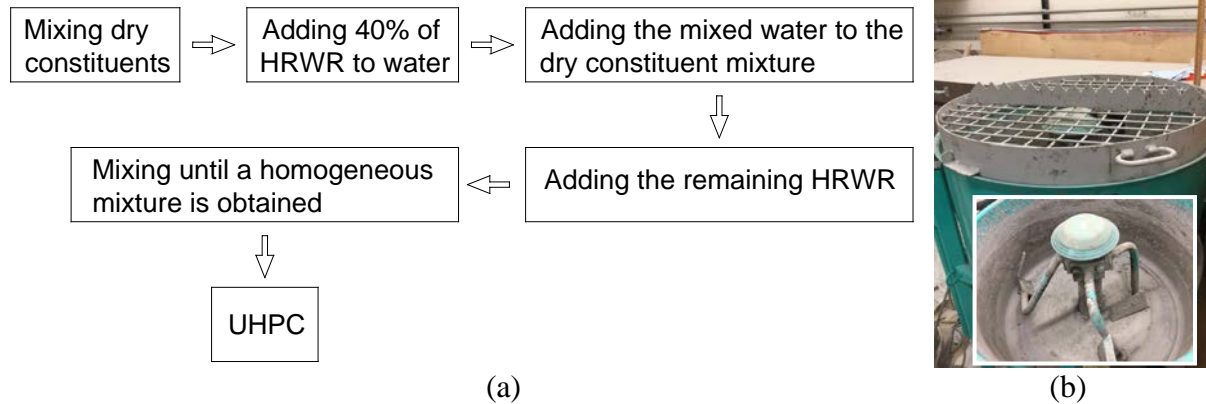


Fig. 2. Mixing procedure: (a) sequence; (b) vertical shaft mixer

2.1.8. Polypropylene fiber

A collated fibrillated form of recycled polypropylene fibers (Table 1 and Fig. 1(d)) were used to reproduce one of the UHPC mixtures proposed by others (to be presented). The expected benefits of these synthetic fibers are the same as those of the above-mentioned steel fibers.

2.2. Mixing procedure

Figure 2(a) illustrates the base mixing procedure of UHPC. All dry constituents were premixed for a uniform distribution in a vertical-shaft mixer at a paddle speed of 38 rpm (Fig. 2(b)). After two minutes of premixing, 40% of the specified HRWR amount (to be detailed) was added to water and gradually poured to the mixer and blended for two minutes. The remaining HRWR was then added to the mixture and the entire concrete ingredients were stirred until a homogeneous mixture was obtained.

Table 3. Overview of experimental program

Test category	Content
I	Reproduction of benchmark mixture designs
II	Assessment of workability by measuring slump
III	Effect of silica fume types

IV	Effect of pyrogenic and precipitated silica products
V	Effect of steel fibers

2.3. Specimen Preparation

Concrete cylinders (4 in. in diameter and 8 in. in depth) and prisms (4 in. by 4 in. by 12 in.) were cast to examine the compressive strength and flexural capacity of various UHPC mixtures, respectively. Bond test specimens were composed of a concrete block (8 in. wide by 8 in. long by 7 in. deep) with a No. 3 steel reinforcing bar, including a bond length of 1 in. (a plastic tube was used to unbond the bar), as shown in Fig. 3. A threefold experimental scheme was used: i) reproduction of benchmark UHPC mixtures proposed by others, ii) development of a prototype UHPC mixture with locally available materials, and iii) experimental parametric investigations. Primary test parameters were silica admixtures, water-cement ratios, workability, and steel and polypropylene fibers. Table 3 summarizes individual categories with a concise description. Category I is composed of nine mixtures selected from literature; Category II evaluates the workability of UHPC mixtures with variable water/cement ratios ($w/c = 0.21$ to 0.23); Categories III and IV assess the implications of silica fume (Types A to D, Table 1) as well as pyrogenic and precipitated silica products (Table 2), respectively; and Category V appraises the compressive and flexural capacities of UHPC with and without steel fibers. As far as the existing nine mixtures are concerned (Table 4), four silica products (silica powder, silica fume, silica sand, and finer silica sand) were used with two reinforcement types (steel and polypropylene fibers), in addition to conventional concrete constituents (water, cement, sand, and HRWR). It should be noted that some ingredients were adjusted because information was not fully disclosed in the references; for example, the amount of HRWR in the No. 3 mixture was modified from 828 oz/yd^3 to 882 oz/yd^3 to satisfy the manufacturer's recommendation. Each test category was replicated five times to attain a mean compressive strength.

2.4. Curing condition

The concrete specimens were cured under moisture and heat conditions, depending upon the scope of the test categories (Table 3) and technical interest in the nine mixtures (Table 4). Because the water/cement ratio of the UHPC mixtures ($w/c = 0.21$ to 0.23) was markedly lower than the ratio of ordinary concrete ($w/c = 0.4$ to 0.5), curing was considered a salient factor influencing the strength of the concrete. ASTM C192 (*Standard practice for making and curing concrete test specimens in the laboratory*, ASTM 2016) was referenced for moisture curing. The specimens were initially covered with plastic sheets and stored in a curing room (73°F at a 99% humidity, on average) for 24 hours.

Table 4. Benchmark UHPC mixtures (Category I)

	Identification of mixture design								
	No. 1 (AM)	No. 2 (MO)	No. 3 (RU)	No. 4 (AS)	No. 5 (ZD)	No. 6 (W)	No. 7 (WI)	No. 8 (AH)	No. 9 (AH)
Water (lb/yd ³)	334	349	184	293	364	264	264	300	276
Cement (lb/yd ³)	1,391	1,517	1,200	1,391	1,506	1,200	1,391	1,304	1,200
Sand (lb/yd ³)	0	1,897	1,720	1,922	0	2,017	1,280	1,770	1,720
Silica powder (lb/yd ³)	0	0	0	0	0	360	348	0	0
Silica fume (lb/yd ³)	209	228	390	305	301	300	348	428	390
Silica sand (lb/yd ³)	1,739	0	356	0	1,220	0	0	374	356
Finer silica sand (lb/yd ³)	0	0	0	0	512	0	0	0	0
HRWR (oz/yd ³)	511	650	882	789	650	1,579	1,579	604	882
Steel fiber (lb/yd ³)	223	270	263	152	0	0	376	301	263
Polypropylene fiber (lb/yd ³)	1.4	0	0	0	0	0	0	0	0

AM = Al Madhoun (2013); MO = Mohammed (2015); RU = Russell and Graybeal (2013); AH = Ahlborn et al. (2008b); AS = Askar et al. (2013); ZD = Zdeb (2013); W = Wille et al. (2011a); WI = Wille et al. (2011b)

After stripping, the cylinders and prisms were submerged in a water tank for moisture curing and relocated to an electric oven for heat curing (194°F), and cured for additional 27 days (a total curing time of 28 days was employed in this research program unless otherwise stated). The heat curing temperature was determined as per published research (Tafraoui et al. 2009; Yang et al. 2009).

2.5. Mechanical testing

Pursuant to ASTM C39 (*Standard test method for compressive strength of cylindrical concrete specimens*, ASTM 2015b), all concrete cylinders were monotonically loaded until failure occurred (Fig. 3(a)). A built-in load cell in the testing machine measured the ultimate load of the cylinders. The prism specimens were subjected to three-point bending (Fig. 3(b)) at a span length of 10 in., as guided by ASTM C1609 (*Standard test method for flexural performance of fiber-reinforced concrete using beam with third-point loading*, ASTM 2012). A load-cell and a linear potentiometer were used to monitor the applied load and the corresponding deflection at midspan, respectively. The digital image correlation (DIC) technique visually examined the initiation and propagation of flexural cracks when the prisms were loaded. The DIC system consisted of a high-resolution camera (5 megapixel), a macro lens, and a computer built with a 3.5 GHz quad core and a 16 GB RAM (Fig. 3(c)). Details of the bond test are provided in Fig. 3(d).

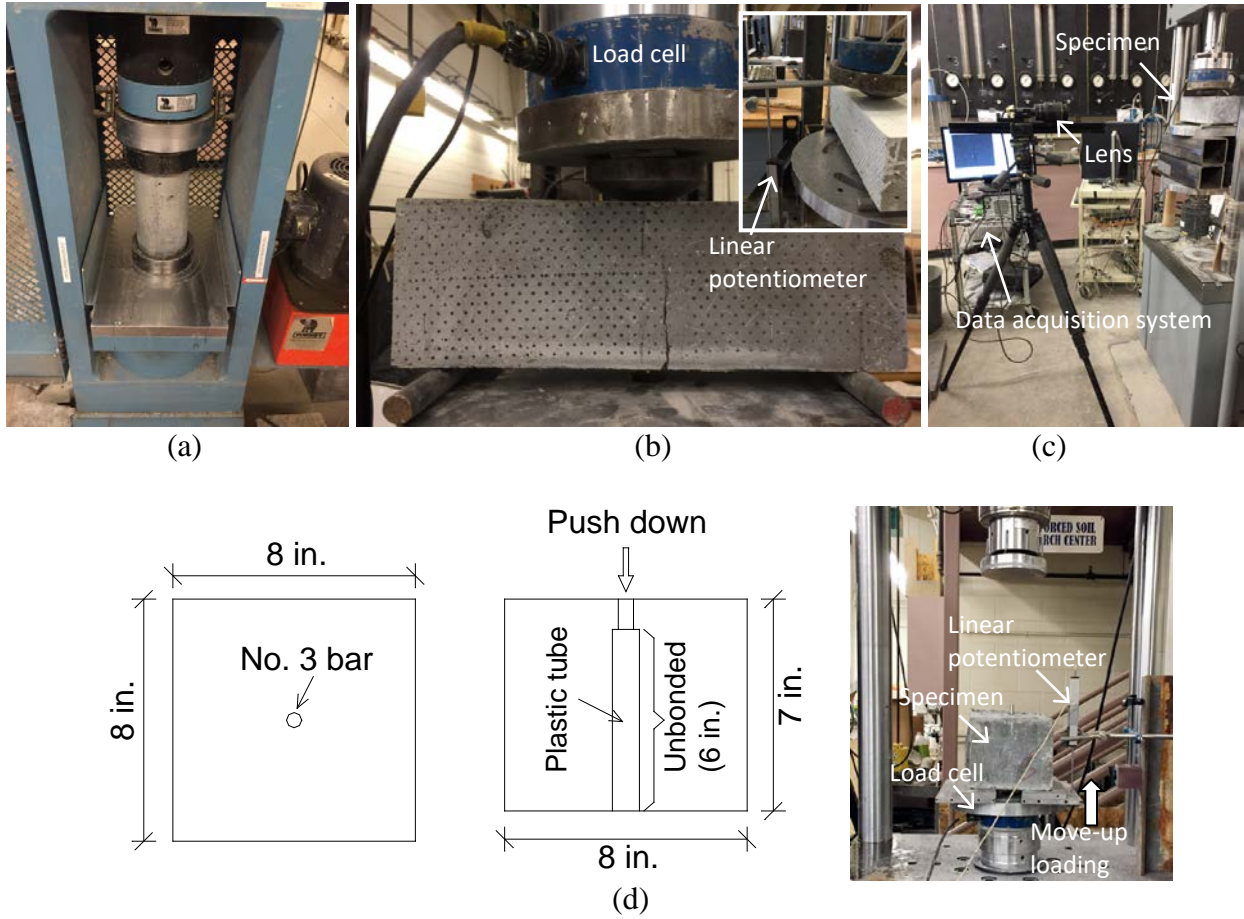


Fig. 3. Test details: (a) compressive test; (b) flexural test; (c) digital image correlation; (d) bond test

3. Experimental Results

A variety of technical data is discussed from material characteristics to implementation details. Experimental parametric investigations examine the effects of constituent types on the strength of UHPC.

3.1. Distribution of particle size

The size distribution of the above-explained granular ingredients in UHPC was quantified by an image processing program (Ferreira and Rashband 2012). Each material was randomly sampled and placed for digital microscopy, as shown in Fig. 4(a). Magnification levels were adjusted up to 900 times magnification, depending upon grain size. After acquiring metadata, the file was converted to black and white for image analysis (Fig. 4(b)). A calibration was conducted with known dimensions to measure the grids of spatial pixel intensities. The data of the individual grains were clustered to establish observation frequencies at a specific size. The mean size of each granular constituent (μ) was determined by

$$\mu = \frac{S_p}{S_d} = \frac{\sum nf}{\sum f} \quad (1)$$

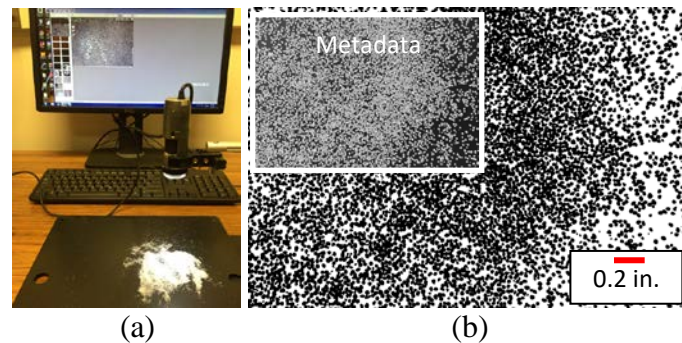


Fig. 4. Image processing for particle distribution: (a) digital microscopy; (b) converted image of silica sand

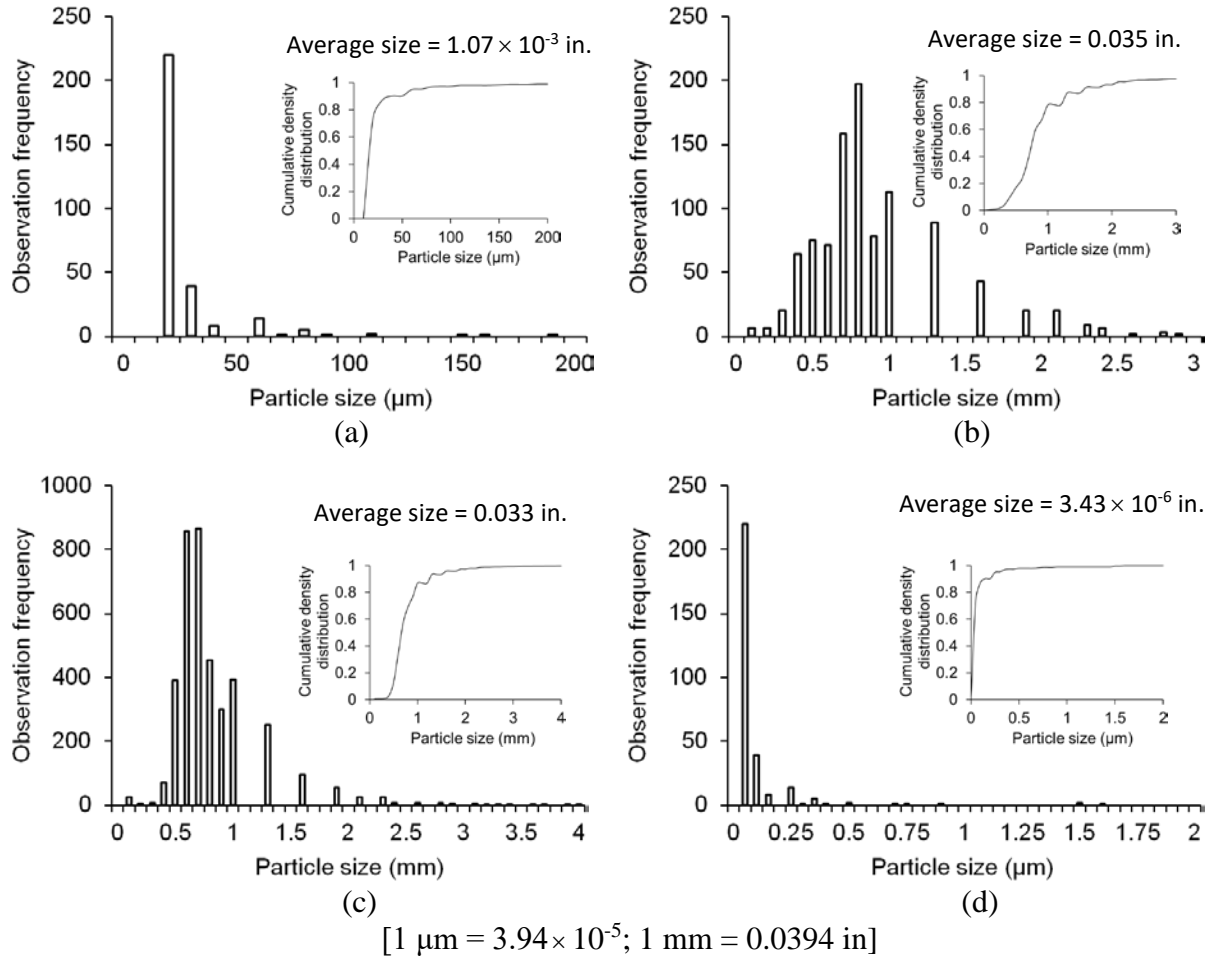


Fig. 5. Particle size distribution: (a) cement; (b) silica sand; (c) finer silica sand; (d) silica fume

where S_p is the product sum of the particle size (n) and observation frequency (f); and S_d is the summation of the observation frequency. Figure 5 plots the distribution of the granular constituents. For cement, more than 92% of the particles were placed between 0.79×10^{-3} and 2.4×10^{-3} in. (Fig. 5(a)), leading to an average size of 1.07×10^{-3} in. The distributions of silica sand (Fig. 5(b)) and finer silica sand (Fig. 5(c)) were dispersed in comparison with that of the cement, owing to the fact that sandstone is disaggregated without fine milling. The average particle size of the silica sand and the finer silica sand was 0.035 in. and 0.033 in., respectively, accompanied by similar cumulative density distribution patterns (insets of Figs. 5(b) and (c)).

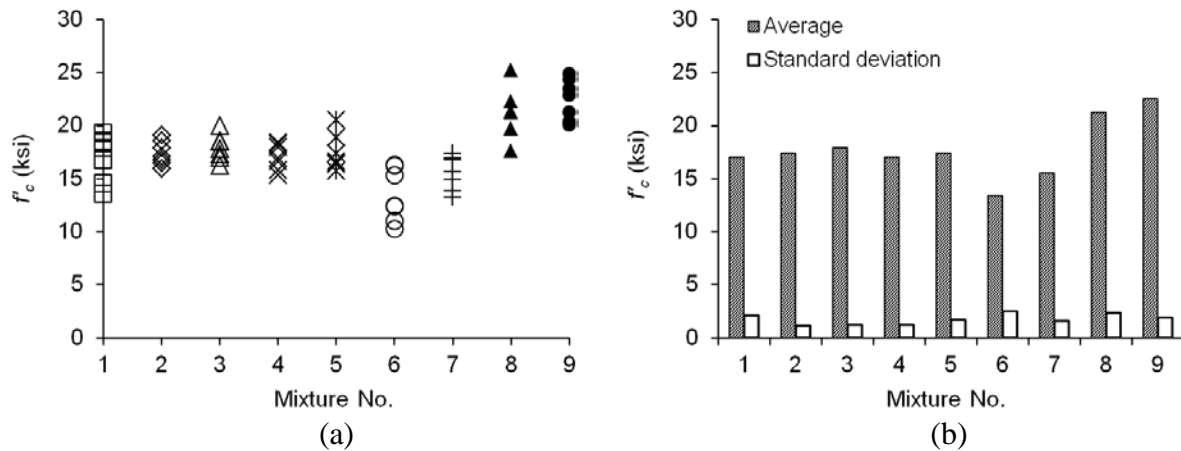


Fig. 6. Reproduction of existing mixtures (Category I): (a) individual; (b) average

These measured distribution characteristics differed from the sieve-analysis-based manufacturers' effective size 0.016 to 0.02 in. for silica sand and 0.006 to 0.012 in. for finer silica sand. The distribution of silica fume (Type D in Table 1) was skewed because of its fine particle nature at an average size of 3.43×10^{-6} in. (Fig. 5(d)).

3.2. Strength of benchmark UHPC mixtures

Figure 6 exhibits the compressive strength of the benchmark mixtures in Category I. The water-cement ratios of the mixtures varied from $w/c = 0.15$ to 0.24: the setting time of the concrete was approximately 50 minutes. It is important to note that the reproduced strengths were not the same as those of the references, because test details were not disclosed in many cases (products and specific curing conditions). Accordingly, the previously mentioned materials purchased for the present study were employed under the generic curing conditions in order to evaluate the effects of the individual ingredients. The average strengths of mixtures No. 1 to No. 5 were similar, ranging from 16.9 ksi to 17.8 ksi. These were higher than the strengths of the No. 6 and No. 7 mixtures 13.3 ksi and 15.5 ksi, respectively). This difference can be ascribed to the inclusion of silica powder (30.1% and 24.9% of the cement mass for the No. 6 and No. 7 mixtures, respectively), and indicates that silica powder may not be recommendable to the formulation of UHPC. The heat curing resulted in higher strengths for the No. 8 and No. 9 mixtures. Despite the positive results of heat curing in terms of strength, such a method may not be practical on site.

Consequently, it was decided that a UHPC mixture would be developed under an ambient temperature condition.

Table 5. Finalized UHPC mixture

<i>w/c</i>	Water (lb/yd ³)	Cement (lb/yd ³)	Silica fume (lb/yd ³)	Finer silica sand (lb/yd ³)	Silica sand (lb/yd ³)	HRWR (oz/yd ³)
0.22	334	1,517	280	512	1,582	557

The concrete cylinders with silica sand (Nos. 1, 3, 5, 8, and 9) generally showed higher strengths than the others. Finer silica also appeared to increase the compressive strength (No. 5). The amount of HRWR was not correlated with the strength, as supported by previous research (Gagne et al. 1996). In other words, the HRWR quantities, ranging from 511 oz/yd³ to 604 oz/yd³, did not appreciably alter the concrete strength. The presence of steel fibers increased the strength, since the fibers impeded the occurrence of random directional cracks when the cylinders were axially loaded (that is, perpendicular to the principle stress directions of the local cracks). The use of polypropylene fibers, by contrast, did not seem to be influential on the strength. Therefore, steel fibers are recommendable for UHPC mixtures.

3.3. Determination of UHPC mixture proportion

Because no standard exists in designing UHPC mixtures, the following procedure was used to develop a prototype mixture (Table 5). A representative value was accepted among the benchmark proportions, unless improvements and adjustments were necessary. Conforming to the test observation of the benchmark mixtures, silica powder and polypropylene fibers were not included. It is also worth noting that, unlike conventional concrete mixtures, air entrainment may not be required for UHPC because its dense configuration with considerably low porosity precludes the ingress of water that causes freeze-thaw damage (Ahlborn et al. 2008a).

3.3.1. Cement

The maximum cement amount of 1,517 lb/yd³ used in the benchmark mixtures was adopted to provide favorable strength, cohesiveness, and finishability of the UHPC. Although greater plastic shrinkage might take place due to the use of a large amount of cement, it would be addressed by moisture curing (prevention of water loss from the mixed concrete during the plastic state).

3.3.2. Water

According to the average ratio of the benchmark mixtures, a water-cement ratio of $w/c = 0.22$ was selected (a preliminary test showed that the low w/c ratios of the benchmark proportions provided dense concrete mixtures with unreasonable workability). The amount of water was thus 334 lb/yd^3 .

3.3.3. Silica fume

The amount of silica fume was determined based on the benchmark mixtures in conjunction with complementary literature. The average ratio of water to cementitious materials (cement plus silica fume) in the benchmark mixtures was $w/cm = 0.17$. Laboratory observations revealed that such a ratio entailed unacceptable workability. Furthermore, the dosage of a high-range water reducer had a certain limit (over-dosage caused softening of the mixed concrete when demolded). Vanderburg and Wille (2018) stated that a water-to-cementitious materials ratio of $w/cm = 0.2$ frequently provided a compressive strength of 22 ksi, which is higher than the target strength of the present study (20 ksi). Accordingly, the average of the above-mentioned ratios was taken ($w/cm = 0.185$), leading to a silica fume amount of 280 lb/yd^3 . It is worthwhile to note that a plethora of silica fume (exceeding a void volume between cement particles) can degrade the strength of concrete, because the cement particles repulse each other (known as the loosening effect, De Larrard 1999).

3.3.4. Finer silica sand

The amount of 512 lb/yd^3 shown in the benchmark mixture was adopted. Since finer silica sand is a constituent supplementary to silica sand, further adjustments were not conducted.

3.3.5. Silica sand

The average ratio between the total sand (natural sand, silica sand, and finer silica sand) and cement of the benchmark mixtures was 1.42. Wille et al. (2011a) reported that a sand-to-cement ratio of 1.38 showed the highest compressive strength when the ratio varied from 1.36 to 1.68. Following this recommendation, the amount of silica sand was determined to be $1,582 \text{ lb/yd}^3$.

Table 6. Mixtures for slump test (Category II)

ID	w/c	Water (lb/yd ³)	Cement (lb/yd ³)	Silica fume (lb/yd ³)	Finer silica sand (lb/yd ³)	Silica sand (lb/yd ³)	HRWR (oz/yd ³)
ST-1	0.23	349	1,517	280	512	1,582	557
ST-2 ^a	0.22	334	1,517	280	512	1,582	557
ST-3	0.21	319	1,517	280	512	1,582	557

^a: ST-2 is the same as the finalized mixture in Table 5

3.3.6. High-range water reducer

The average amount of HRWR used in the benchmark mixtures was 917 oz/yd³, which was higher than the average dosage of 189 oz/yd³ in the selected HRWR product. The average of these two values was hence adopted: 557 oz/yd³. It is noted that the amount of HRWR generally does not influence the strength of concrete (Neville 1995).

3.3.7. Steel fiber

The benchmark mixtures provided an average steel-fiber amount of 2.0% (the fiber mass divided by its density of 490 lb/ft³). An experimental parametric study showed that the fiber inclusion of 2% and 3% was best in terms of compressive strength and bond performance, respectively (Yoo et al. 2013). The average of these values resulted in 2.3%, which is equivalent to 303 lb/yd³.

3.4. Parametric investigations

Based on the above-described prototype UHPC mixture design, a parametric study was conducted to examine the effects of individual constituents.

3.4.1. Workability

A comparison of slump between the mixtures with natural sand and silica sand is given in Fig. 7(a). The concrete with the silica sand exhibited a 398% higher slump than that with the natural sand, which confirms the former's superior rheological characteristics. Figure 7(b) shows the slump of the Category II mixtures specified in Table 6, where three water-cement ratios of $w/c = 0.21, 0.22,$ and 0.23 are comparatively listed (the silica fume used was Type D in Table 1). The mixtures with water-cement ratios of $w/c = 0.22$ and 0.23 revealed a slump of 203 mm (8 in.), as pictured in Fig. 7(b); however, the mixture with a water-cement ratio of $w/c = 0.21$ provided a

63% lower slump (3 in.). Considering the constructability of the dense UHPC mixtures, the slump of 3 in., similar to that of ordinary concrete, may not be acceptable for practice.

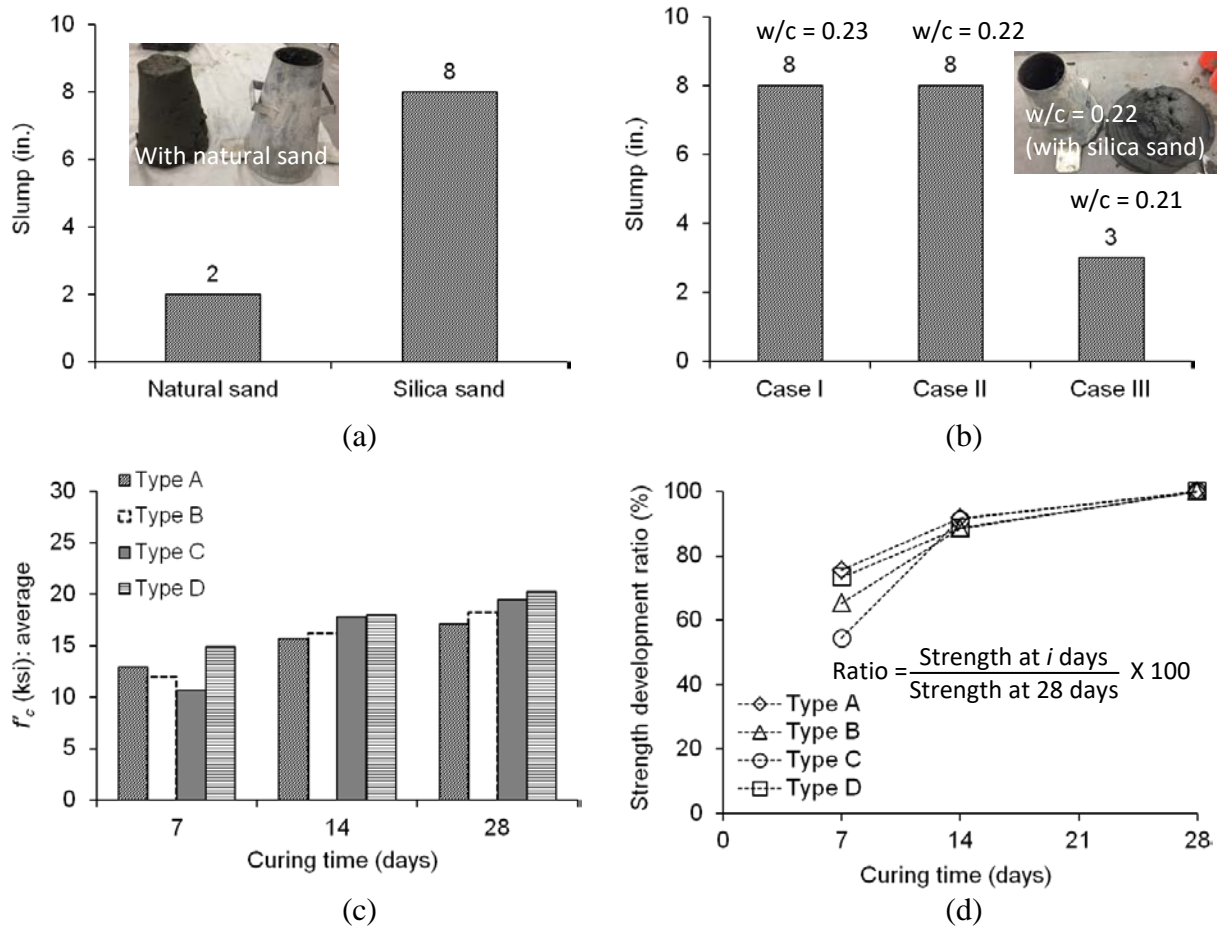


Fig. 7. Experimental parametric study: (a) effect of silica sand; (b) assessment of workability (Category II); (c) effect of silica fume types (Category III); (d) strength development dependent upon silica fume types (Category III)

3.4.2. Silica fume type

Four types of silica fumes (Types A to D, Table 1) were employed for the Category III mixtures. The primary differences among these silica fume products were the amount of SiO₂ (85% to 98%) and bulk density (19 to 38 lb/ft³). The concrete mixtures were moisture cured at room temperature prior to testing at 7, 14, and 28 days. The average strength of the mixtures increased with curing time, whereas the strength-gain pattern was influenced by the type of silica fume (Fig. 7(c)). The average strength of the mixtures with Type D was consistently higher than the

strength of those with other silica fume types. This observation indicates that the content of SiO_2 was a crucial factor controlling the compressive strength of UHPC (SiO_2 of Type D was 98%, while that of the other types was 85%). It is known that SiO_2 reacts with $\text{Ca}(\text{OH})_2$ to form pozzolanic calcium silicate hydrate (C-S-H), which enhances the bond between the cement particles (Strunge and Deuse 2008), thereby increasing the compressive strength of the concrete. The bulk density of the silica fume affected strength development ratios at an early stage, as shown in Fig. 7(d) where the individual strength was divided by the strength at 28 days for comparison. When the bulk density of the silica fume was high, the compressive strength of the concrete mixtures at 7 days became low. For instance, the mixture with Type C (bulk density = 38 lb/ft^3) showed an average strength development ratio of 54.4%, which was lower than the mixtures with Types B and D (bulk density = 30 lb/ft^3 and 19 lb/ft^3 , respectively). Despite the absence of a bulk density in Type A (the manufacturer's data sheet does not provide details), it can be conjectured that the densities of Types A and D were analogous since their 7-day responses were close (75.6% and 73.4%, respectively, in Fig. 7(d)). The strength development ratios of all these mixtures became similar at 14 days and were almost the same at 28 days. It is thus conclusively stated that the properties of the silica fume altered the strength of the UHPC mixtures; however, its development rate after 7 days was virtually independent of those properties.

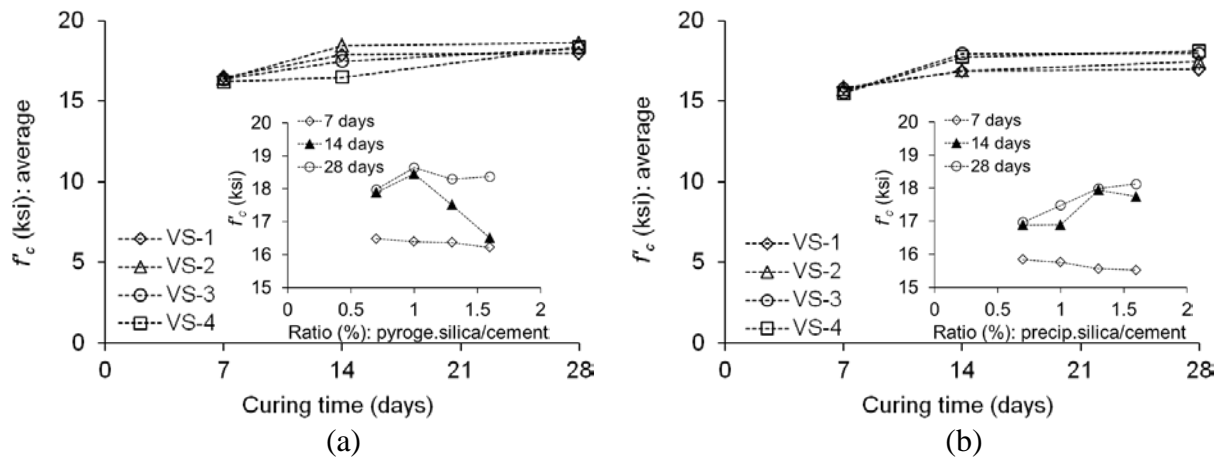


Fig. 8. Effect of pyrogenic/precipitated silica (Category IV): (a) mixture with pyrogenic silica; (b) mixture with precipitated silica

3.4.3. Pyrogenic/precipitated silica

Figure 8 shows the implications of pyrogenic and precipitated silica products on the strength development of the Category IV concrete mixtures (Table 7) measured at 7-day to 28-day curing periods. The four test groups (VS-1 to VS-4) indicate the ratio of pyrogenic/precipitated silica to cement, varying from 0.7% to 1.6% (Table 7). The 7-day strength of the mixtures with the pyrogenic silica (16.2 ksi) was 3.7% higher than that of the mixtures with the precipitated silica (15.7 ksi), on average. As the curing period increased, bifurcations were noticed contingent upon the silica-cement ratio. In the case of the pyrogenic silica (Fig. 8(a)), the 14-day strength revealed a decreasing propensity with an increase in the silica-cement ratio (for example, the average strengths of VS-1 (ratio = 0.7%) and VS-4 (ratio = 1.6%) were 17.8 ksi and 16.4 ksi, respectively); afterward, all responses converged to an average strength of 18.3 ksi at 28 days (Fig. 8(a)). The mixtures with precipitated silica exhibited two apparent branches at 14 and 28 days (Fig. 8(b)). The responses of VS-1 and VS-2 were alike (average strength of 17.1 ksi) and the responses of VS-3 and VS-4 were clustered (average strength of 18.0 ksi). This trend indicates that the strength of the mixtures (14 and 28 days) with precipitated silica tended to rise with the increased silica-cement ratio (Fig. 8(b)). Given that the 28-day strengths of the mixtures with the pyrogenic and precipitated silica products were 18.3 ksi and 17.7 ksi respectively, which is lower than the target strength of 20 ksi, these materials may not be recommendable for the formulation of UHPC mixtures.

Table 7. Mixtures with various pyrogenic/precipitated silica admixtures (Category IV)

	<i>w/c</i>	Water (lb/yd ³)	Cement (lb/yd ³)	Silica fume (lb/yd ³)	Finer silica sand (lb/yd ³)	Silica sand (lb/yd ³)	HRWR (oz/yd ³)	Pyrogenic/ precipitated silica (lb/yd ³)
VS-1	0.22	334	1,517	285	512	1,582	557	1
VS-2 ^a	0.22	198 (334)	1,517	280	512	1,582	557	15
VS-3	0.22	198 (334)	1,517	276	512	1,582	557	20
VS-4	0.22	198 (334)	1,517	271	512	1,582	557	24

^a: VS-2 is the same as the finalized mixture design in Table 5 except for pyrogenic/precipitated silica

Table 8. Mixtures with/without steel fiber (Category V)

	w/c	Water (lb/yd ³)	Cement (lb/yd ³)	Silica fume (lb/yd ³)	Silica sand (lb/yd ³)	Finer silica sand (lb/yd ³)	HRWR (oz/yd ³)	Steel fiber (lb/yd ³)
BT-1 ^a	0.22	334	1,517	280	1,582	512	557	0
BT-2	0.22	334	1,517	280	1,582	512	1,068	303

^a: BT-1 is the same as the finalized mixture in Table 5

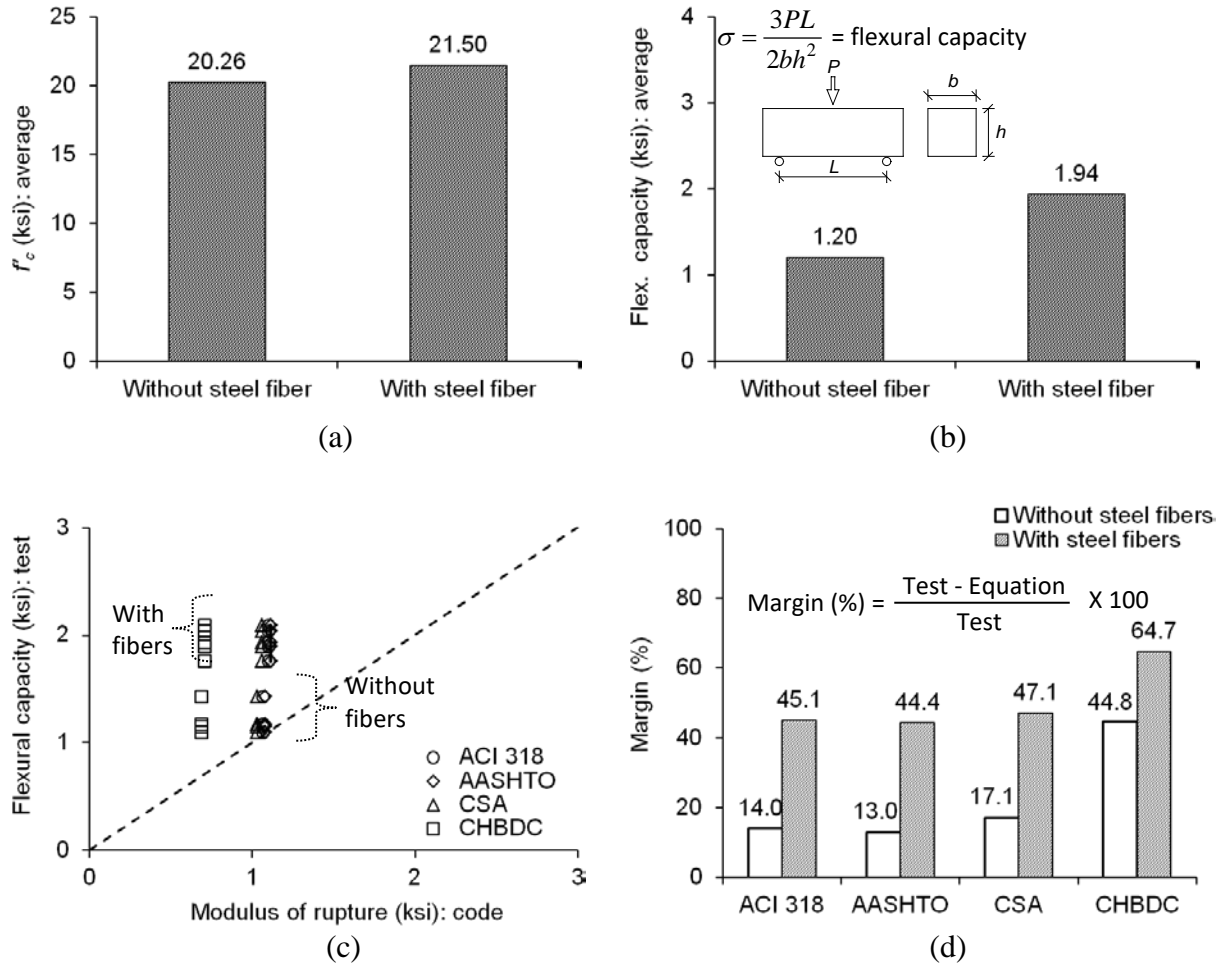


Fig. 9. Assessment of modulus of rupture expressions (Category V): (a) compressive strength; (b) flexural capacity; (c) capacity comparison with and without steel fibers; (d) assessment of code expressions

3.4.4. Strength with steel fibers

The compressive strength and flexural capacity of the mixtures with and without steel fibers (Table 8, Category V) are shown in Figs. 9(a) and (b), respectively. The compressive strength of the fiber-mixed concrete was 6.1% higher than that of the plain concrete (Fig. 9(a)), on average, due to the fibers' resistance to the formation of local cracks. The inclusion of the fibers increased the flexural capacity by 60.5% (Fig. 9(b)). These observations signify that steel fibers can be added to the proposed UHPC mixture (Table 5) when members are subjected to flexural loading (or with apparent eccentric loading). Figures 9(c) and (d) evaluate the applicability of code equations concerning the modulus of rupture (f_r) with the compressive strength of the individual concrete cylinders (f'_c in Fig. 9(a): f_r is a function of f'_c). While the code expressions were generally conservative, the margins of ACI 318 (ACI 2014) and AASHTO (AASHTO 2017) equations against the average test value (14.0% and 13.0%, respectively) were lower than those of the CSA (CSA 2010) and CHBDC (CHBDC 2014) equations (17.1% and 44.8%, respectively). As the steel fibers were mixed with the concrete, the margins of the equations increased to 45.1% (ACI 318), 44.5% (AASHTO), 47.1% (CSA), and 64.7% (CHBDC). These discrepancies are attributed to the empirical nature of the code equations, which were calibrated with ordinary concrete.

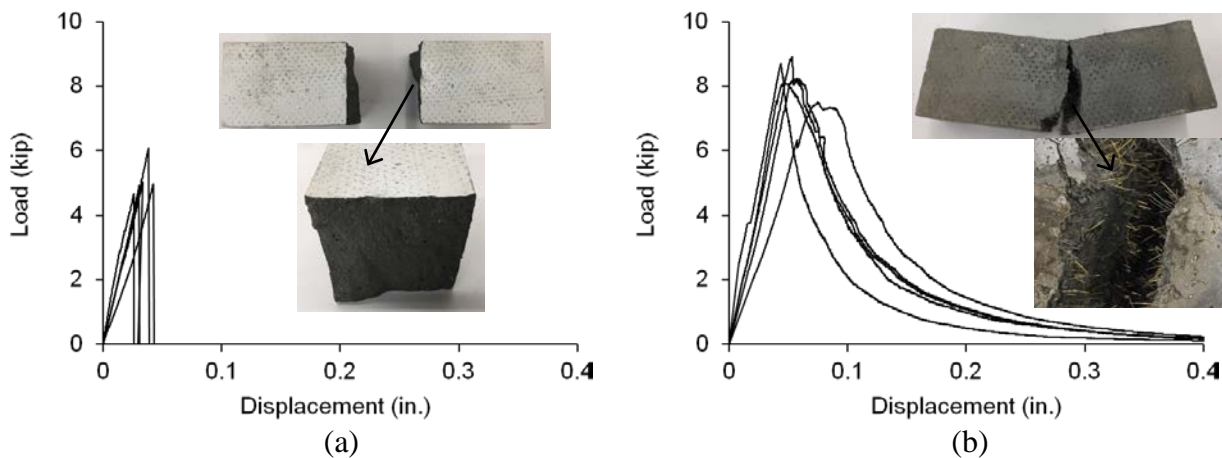
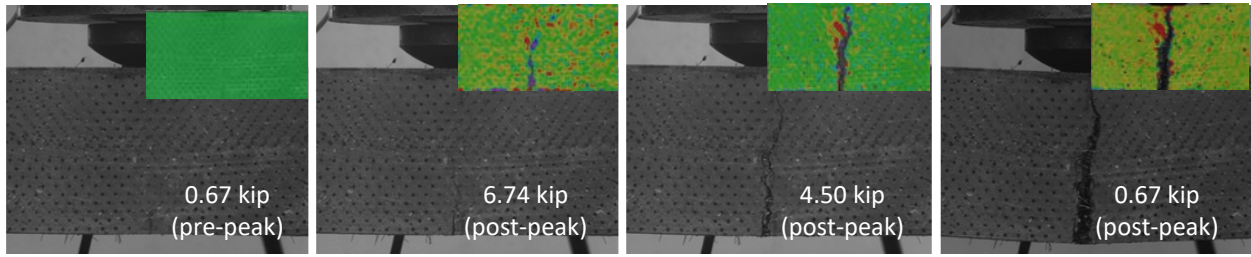
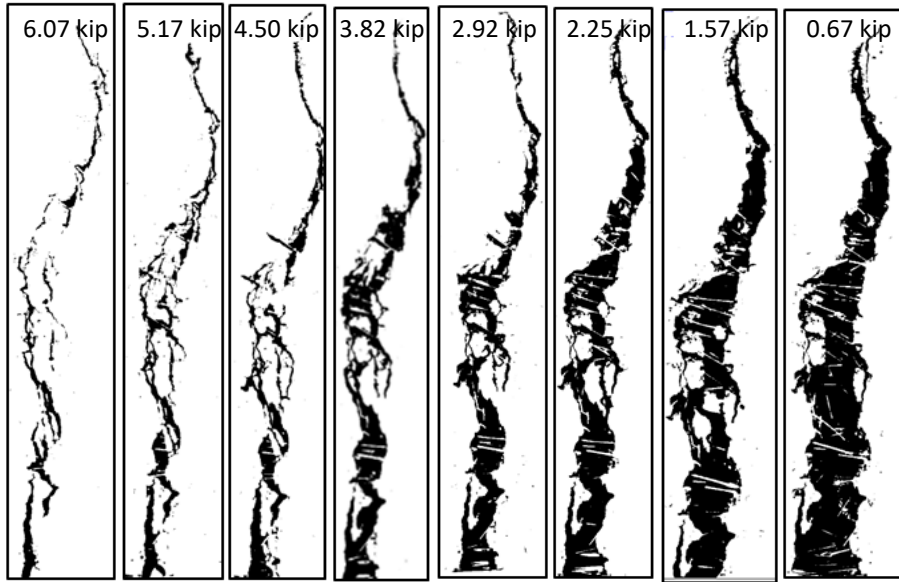


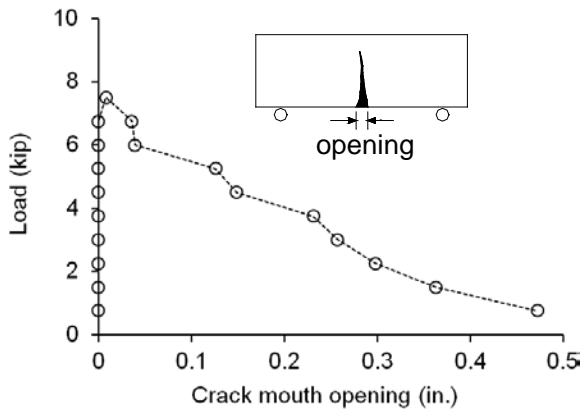
Fig. 10. Load-displacement of UHPC prisms (Category V): (a) without steel fibers; (b) with steel fibers



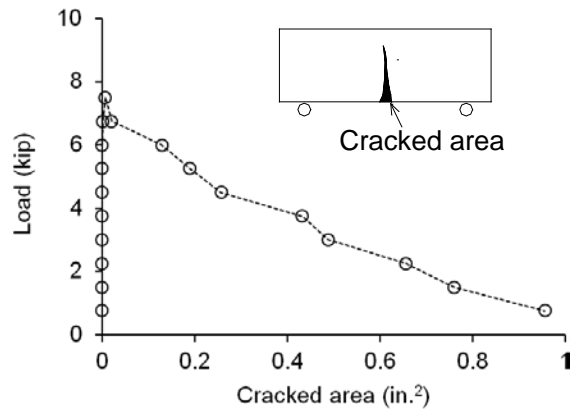
(a)



(b)



(c)



(d)

Fig. 11. Crack development of specimen with steel fibers: (a) view of cracking; (b) post-peak propagation at midspan; (c) load-crack mouth opening; (d) load-cracked area

3.5. Crack development

Figure 10 compares the load-displacement behavior of the prisms with and without the steel fibers. Both test groups revealed a linearly increasing trend up to the peak loads, after which the specimens without the fibers failed abruptly (Fig. 10(a)), and those with the fibers demonstrated gradual post-peak responses caused by the fiber-induced crack resistance (Fig. 10(b), inset). The initiation and progression of cracks in the fiber-mixed concrete are pictured in Fig. 11(a). Owing to the brittle failure, sequential snapshots were not available for the prisms without the fibers. Figure 11(b) provides the details of post-peak crack propagation monitored by an image processing program (ImageJ, Ferreira and Rashband 2012). The crack initiated at a pre-peak load of 6.7 kips and developed until the specimen failed, as shown in Fig. 11(c). The cracked area of the concrete revealed an almost linearly increasing pattern with the post-peak load (Fig. 11(d)), which can explain the energy dissipation characteristics of the UHPC mixed with the steel fibers subjected to flexural loading.

3.6. Modulus of rupture

To complement the prism test results, Monte Carlo simulations were conducted for the cases with and without steel fibers. This random sampling technique is useful to numerically create statistical data when experimental outcomes are limited:

$$z_i = \Phi^{-1}(x_i) \quad (2)$$

$$s_i = \mu_{\text{exp}} + z_i \sigma_{\text{exp}} \quad (3)$$

where z_i is the standard normal random value; $\Phi^{-1}(\bullet)$ is the inverse of the standard normal cumulative distribution function; x_i is a random variable; s_i is the sampled outcome ($s_i = \text{either } f'_c \text{ or } f_r$); and μ_{exp} and σ_{exp} are the mean and standard deviation of the test data associated with the outcome, respectively. A normality test was performed with the following equation:

$$z_i = \Phi^{-1}\left(\frac{E - a}{k + 1 - 2j}\right) \quad (4)$$

where E is the sorted test data for either the compressive strength (f'_c) or the maximum flexural capacity (σ_{max}); k is the total number of the test ($k = 5$ for the individual case); and j is a constant ($j = 0.375$ for $k \leq 10$). Figure 12(a) exhibits the linearly increasing z_i with an increase in the f'_c and σ_{max} values, which indicates that the probability distribution of these variables was Gaussian. A total of 40,000 data points were randomly generated for each case using the Monte Carlo method (f'_c and f_r with and without the fibers, respectively), as plotted in Fig. 12(b). The conventional expression for the modulus of rupture was taken and calibrated:

$$f_r = a\sqrt{f'_c} \quad (5)$$

where a is an empirical constant. The variation range of the a constant was from 7.5 to 10.5 (without fibers) and from 12 to 16 (with fibers), covering most of the simulated data sets.

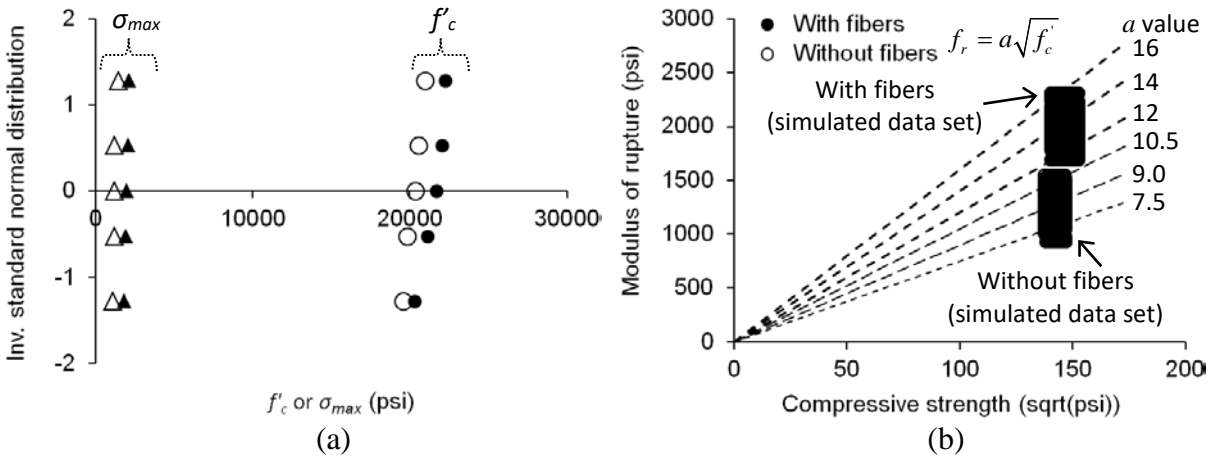


Fig. 12. Modulus of rupture expression with Monte Carlo simulation (sqrt = square root): (a) normality test; (b) determination of empirical constant

The succeeding expression was then recommended to determine the modulus of rupture for the proposed UHPC mixture:

$$f_r = \begin{cases} 9\sqrt{f'_c} & \text{without steel fibers in psi} \\ 14\sqrt{f'_c} & \text{with steel fibers in psi} \end{cases} \quad (6)$$

The margin of the proposed expressions was 3.6% and 1.4% for the concrete without and with the steel fibers, respectively, which was significantly lower than those of the existing code expressions (Fig. 9(d)).

3.7. Bond and Development Length

Figures 13(a) and (b) show the load-displacement behavior of the bond-test specimens without and with steel fibers, respectively. The loads precipitously increased up to the peaks, beyond which abrupt drops were noticed because of bond failure. The frictional resistance of the reinforcement accompanied by mechanical interlock maintained a post-peak load level of about 2 kips. Albeit marginal, the presence of the steel fibers resulted in more displacement (Fig. 13(b)). This fact can be explained by the fact that the randomly mixed fibers protruded from the substrate; as a result, the bond between the concrete and rebar was interrupted. The average bond capacity of the interface (m) was calculated using Eq. 7 and is shown in Fig. 13(c).

$$m = \frac{P_u}{\rho d_b l_b} \quad (7)$$

where P_u is the ultimate load of the interface; and d_b and l_b are the bar diameter and bonded length, respectively. The bond capacity of the specimens without steel fibers was 7.33 ksi, on average, which is 7.2% higher than that of the specimens with the fibers. For comparison purposes, the development length (l_d) of AASHTO (AASHTO 2017) was converted to the average bond stress:

$$l_d = \frac{0.63 d_b f_y}{\sqrt{f_c}} \text{ or } 0.3 d_b f_y \quad (8)$$

$$m = \frac{A_s f_y}{\rho l_d d_b} \quad (9)$$

where f_y is the yield strength of the reinforcement ($f_y = 60$ ksi). Since the compressive strength of the UHPC is greater than $f'_c = 4.41$ ksi, the second expression ($l_d = 0.3d_b f_y$) controls. Substituting Eq. 8 to Eq. 9, the AASHTO-based bond strength becomes:

$$m = \frac{A_s}{0.3pd_b^2} \quad (10)$$

As shown in Fig. 13(d), the bond capacities of the UHPC without and with the fibers were 8.8 and 8.2 times higher than that of AASHTO, respectively. The development length of the UHPC should, therefore, be reduced: as per the present test data, the length can be estimated $2.0d_b$ to $2.2d_b$ based on Eq. 9, which needs further examinations in future research.

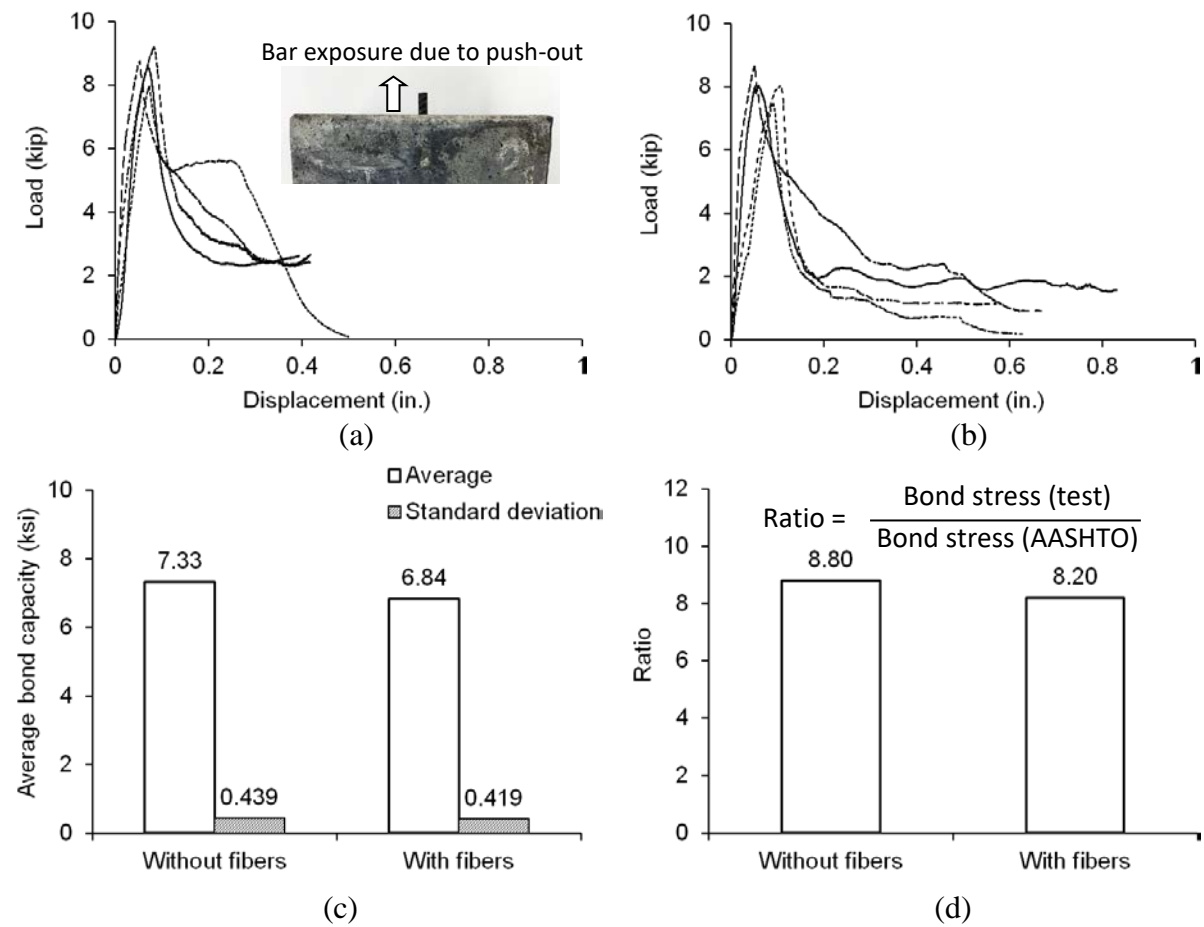


Fig. 13. Bond test results with No. 3 bar: (a) specimens without steel fibers; (b) specimens with steel fibers; (c) average bond stress; (d) comparison with AASHTO LRFD

4. Cost Analysis

Local market prices for the constituents of the developed UHPC are shown in Fig. 14(a). The material costs of the mixtures with and without steel fibers were \$2,573/yd³ and \$1,535/yd³, respectively, assuming that water did not contribute to the total cost. These were up to 74% lower than the cost of commercial products ranging from \$3,270/yd³ to \$5,886/yd³ (Perry and Seibert 2011). Figures 14(b) and (c) detail the breakdown of the total material costs. For the concrete without steel fibers (Fig. 14(b)), finer silica sand and silica sand were the major constituents (27.0% and 24.7% of the total cost), followed by cement (21.9%), silica fume (18.7%), and HRWR (7.8%). These cost proportions altered with the inclusion of the steel fibers, which accounted for 40.3% of the total cost (Fig. 14(c)).

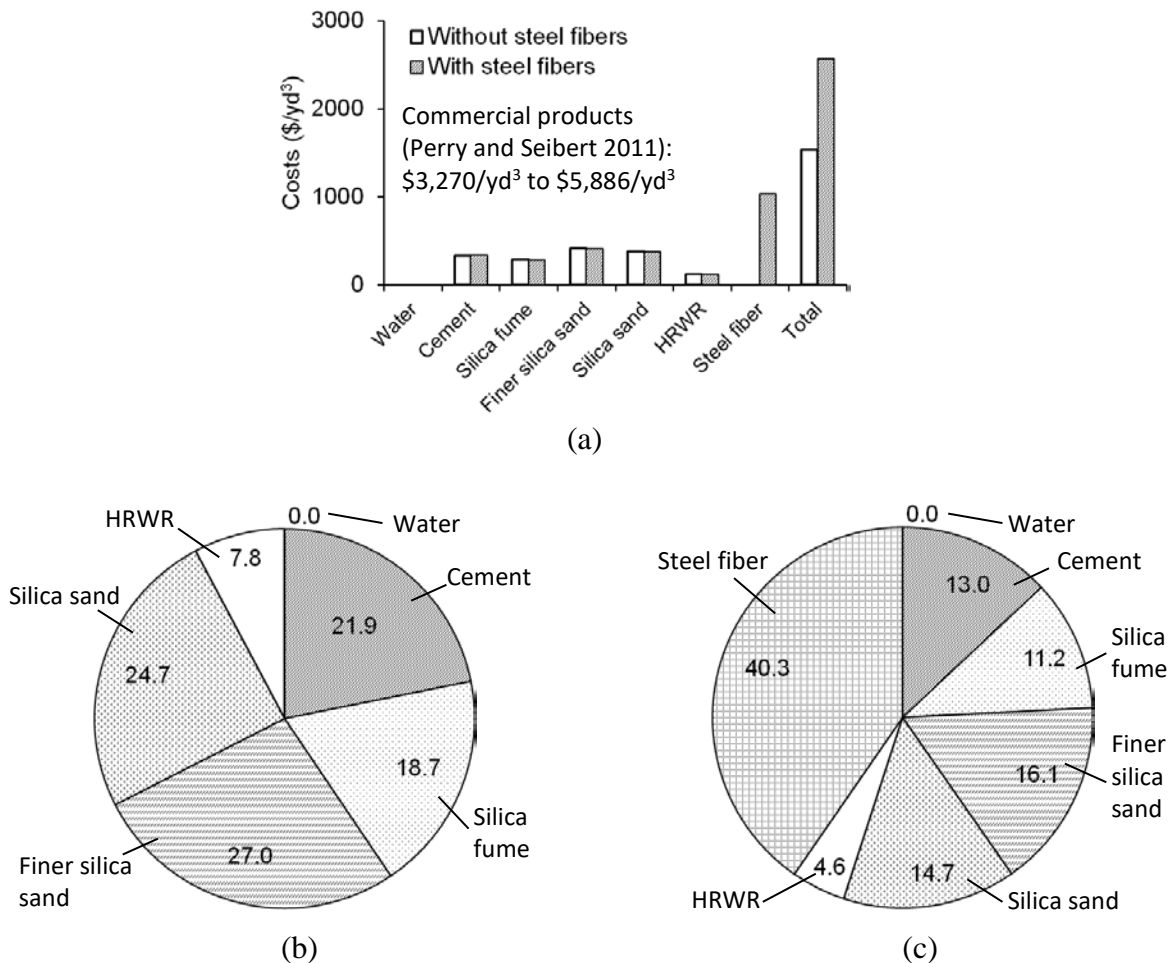


Fig. 14. Cost analysis: (a) materials; (b) cost breakdown percentage without steel fibers; (c) cost breakdown percentage with steel fibers

5. Implementation Plan and Quality Assurance/Control

The consistent quality of UHPC is salient to warrant the sustainable performance of bridge members in Colorado. It is thus important to produce UHPC in accordance with the proposed mixture design, which requires appropriate procedures for quality assurance and quality control. In other words, the material properties described in this report should be referenced to cast reliable UHPC; in other words, CDOT needs to rigorously examine the properties of locally-available materials when planning UHPC-based construction. The selection of inadequate materials may result in unacceptable concrete quality, accompanied by a low strength product. Quality assurance is a systematic endeavor to prevent the potential production of low quality UHPC. The above-employed ASTM standards are recommended to ensure the required strength of concrete in conjunction with the material characteristics specified in the present research program. Because the scale of UHPC to be cast on site is much larger than that of the current experimental program, statistical analysis based on random sampling is inevitable to control the quality of the in-situ UHPC, which is also beneficial for saving operating expenses. Control charts offer an effective and easy way to assess the quality of UHPC products. The concept of the control chart is built upon the probability of occurrence. The following control criteria are recommended for CDOT to implement

$$R = \mu \pm k\sigma \quad (7)$$

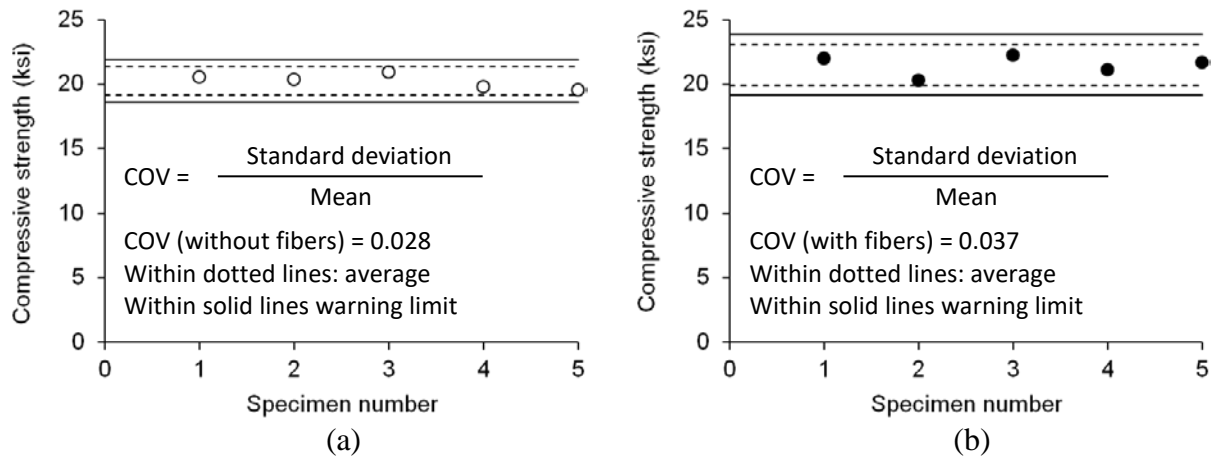


Fig. 15. Control charts for quality control with the finalized UHPC mixture: (a) concrete without steel fibers; (b) concrete with steel fibers

where R is the performance range; μ and σ are the mean and the standard deviation of the samples, respectively; and k is a constant. Three limit categories can be associated with Eq. 7, depending upon k values (Keifer 1981): $k = 1$ (average), $k = 2$ (warning limit), and $k = 3$ (action limit). In accordance with the Gaussian distribution, occurrence probabilities corresponding to the k values are 68.27% for $k = 1$, 95.45% for $k = 2$, and 99.73% for $k = 3$. Figure 15 shows control charts for the concrete with and without steel fibers. The control lines were added as per the experimental (laboratory-obtained) coefficients of variations (COV = standard deviation divided by mean; COV = 0.028 and 0.037 for the concrete specimens without and with fibers, respectively), which are more stringent than typical COV values used on site. For practice, COV = 0.11 may be used (Nowak and Collins 2013). A step-by-step procedure is suggested to formulate the proposed UHPC mixture:

- Step 1: Determine the type of application requiring a specified compressive strength of 20 ksi
- Step 2: Calculate the amount of UHPC necessary for the application
- Step 3: Search for locally available materials
- Step 4: Compare the properties of the identified materials with those enumerated in this report (e.g., silica sand: $\text{SiO}_2 = 90.3\%$, specific gravity = 2.62, and pH = 7.0), as part of quality assurance
- Step 5: Consider whether steel fibers are needed, depending upon the nature of the application
- Step 6: Mix the constituents as guided in this report
- Step 7: Cast trial-batch cylinders to evaluate the properties (quality control)
- Step 8: Use the UHPC mixture

6. Summary and Conclusions

This study has developed cost-effective ultra-high performance concrete (UHPC) using locally available materials to achieve a specified compressive strength of $f'_c = 20$ ksi. A prototype UHPC mixture was formulated based on a combination of nine existing UHPC designs taken from literature with modifications when necessary. The properties of various constituents were examined and the effects were experimentally evaluated. A step-by-step implementation procedure alongside quality assurance/control was proposed for CDOT to employ the developed UHPC in bridge construction. The following conclusions are drawn:

- The microscopy-based distribution of granular particles characterized the size of the individual constituents, which was necessary to understand the micro-void-filling characteristics of the proposed UHPC.
- Tests with the nine benchmark mixtures demonstrated that silica sand and finer silica sand were recommendable to improve the compressive strength of UHPC, rather than silica powder. Heat curing resulted in a better strength gain compared with moisture curing; nonetheless, the latter was adopted owing to the impracticality or difficulty of the former in the field. The amount of high-range water reducers was not influential on the strength of the UHPC within a range varying from 511 oz/yd³ to 604 oz/yd³. Steel fibers performed better than polypropylene fibers. All these findings were integrated to develop the prototype UHPC mixture in tandem with supplementary literature.
- The performance of the developed UHPC at a water-cement ratio of $w/c = 0.22$ was satisfactory in terms of workability (slump = 8 in.) and compressive strength ($f'_c = 20.3$ ksi and 21.5 ksi without and with steel fibers, respectively, on average). The inclusion of steel fibers enhanced the flexural capacity of the UHPC (an average increase of 60.5% relative to the concrete without fibers).
- The amount of SiO₂ in silica fume was an important factor for altering the concrete strength by creating pozzolanic calcium silicate hydrate. As the bulk density of silica fume increased, the 7-day strength of the concrete decreased. The strength-gain trend was, however, unaffected by the bulk density after 7 days. Pyrogenic and precipitated silica products were not recommended for UHPC.

- The modulus of rupture equations specified in codes were generally conservative for the developed UHPC (ACI 318 and AASHTO exhibited lower margins than CSA and CHBDC). When steel fibers were included, the code expressions substantially deviated from the test data up to 64.7%. New modulus of rupture equations, which were calibrated with a random sampling technique, were suggested to address this issue.
- The concrete prisms without steel fibers failed abruptly when loaded in flexure, whereas those with the fibers showed gradual load-softening accompanied by particular energy dissipation characteristics (that is, linearly increasing cracked-areas with a decreasing post-peak load).
- The average bond capacity of the UHPC-concrete interface was influenced by steel fibers. The capacity of the specimens without the fibers was 7.2% higher than that of the specimens with the fibers. The development length of the UHPC was shorter than the requirement of AASHTO LRFD Bridge Design Specifications.
- The costs of the developed UHPC mixture were up to 74% lower than the cost of commercial products (this comparison is based on an article published in 2011). As far as the constituents are concerned, finer silica sand and silica sand accounted for 51.7% of the total cost. When mixing with steel fibers, their portion was 40.3% of the total cost with 30.8% of the finer silica sand and silica sand.
- Quality assurance can be accomplished by adhering to the suggested material properties and by testing the concrete pursuant to relevant ASTM standards. Regarding quality control, trial batches should be cast and the concrete strength is appraised using control charts in compliance with the recommended control criteria.

As follow-up research, the applicability of the developed UHPC mixture should be examined. Closure joints between precast girders are a common and easy practice (Appendix B). Technical topics such as shrinkage, hydration, and development length also need to be studied. Upon confirmation, the mixture can be employed for various types of bridge members.

7. References

AASHTO. 2017. AASHTO LRFD Bridge Design Specifications (8th Edition), American Association of State Highway Transportation Officials, Washington, D.C.

ACI. 2014. Building code requirements for structural concrete and commentary (ACI318-14), American Concrete Institute, Farmington Hills, MI.

Ahlborn, T.M., Mission, D.L., Peuse, E.J., and Gilbertson, C.G. 2008a. Durability and strength characterization of ultra-high performance concrete under variable curing regimes, Second International Symposium on Ultra High Performance Concrete, 197-204.

Ahlborn, T.M., Peuse, E.J., Misson, D.L. 2008b. Ultra-high performance concrete for Michigan bridges, material performance Phase 1, Center for Structural Durability, Michigan Technological University, Final Report RC-1525.

Al Madhoun, A.T. 2013. Mechanical properties of ultra-high performance fiber reinforced self-compacting concrete, MS thesis, Islamic University of Gaza, Gaza, Palestine.

Askar, L.K., Tayeh, B.A., and Bakar, B.H.A. 2013. Effect of different curing conditions on the mechanical properties of UHPFC, Iranian Journal of Energy and Environment, 4, 299-303.

ASTM. 2012. Standard test method for flexural performance of fiber-reinforced concrete using beam with third-point loading (ASTM C1609), American Society for Testing and Materials, West Conshohocken, PA.

ASTM. 2015a. Standard specification for silica fume used in cementitious mixtures (ASTM C1240), American Society for Testing and Materials, West Conshohocken, PA.

ASTM. 2015b. Standard test method for compressive strength of cylindrical concrete specimens (ASTM C39), American Society for Testing and Materials, West Conshohocken, PA.

ASTM. 2016. Standard practice for making and curing concrete test specimens in the laboratory (ASTM C192), American Society for Testing and Materials, West Conshohocken, PA.

ASTM. 2017. Standard specification for portland cement (ASTM C150-17), American Society for Testing and Materials, West Conshohocken, PA.

Blais, P. and Couture, M. 1999. Precast, prestressed pedestrian bridge- world's first reactive powder concrete structure, PCI Journal, 44(5), 60-71.

CHBDC. 2014. Canadian highway bridge design code (S6-14), CSA Group, Mississauga, On, Canada.

CSA. 2010. Design of concrete structure (CAN/CSA-A23.3-04), CSA Group, Mississauga, On, Canada.

De Larrard, F. 1999. Concrete mixture proportioning a scientific approach, E & FN Spon, London, UK.

Ferreira, T. and Rashband, W. 2012. The ImageJ user guide, National Institute of Health, Bethesda, MD.

FHWA. 2011. Tech note: ultra-high performance concrete, FHWA-HRT-11-038, Federal Highway Administration, Washington, D.C.

Gagne, R., Boisvert, A., and Pigeon, M. 1996. Effect of superplasticizer dosage on mechanical properties, permeability, and freeze-thaw durability of high-strength concretes with and without silica fume, ACI Materials Journal, 93(2), 111-120.

Garrett, P.R. 1993. Defoaming: theory and industrial applications, Marcel Dekker, Inc. New York, NY.

Graybeal, B.A. 2006. Material property characterization of ultra-high performance concrete, FHWA-HRT-06-103, Federal Highway Administration, Washington, D.C.

Habbaba, A., Lange, A., and Plank, J. 2013. Synthesis and performance of a modified polycarboxylate dispersant for concrete possessing enhanced cement compatibility, *Journal of Applied Polymer Science*, 129, 346-353.

Keifer, O. 1981. Control charts catch changes: can cut costs, *Concrete International*, 3(11), 12-16.

Mehta, P.K. and Monteiro, P.J.M. 2014. *Concrete: microstructure, properties, and materials*, McGraw Hill, New York, NY.

Mohammed, H. 2015, *Mechanical properties of ultra-high strength fiber reinforced concrete*, MS Thesis, University of Akron, Akron, OH.

Neville, A. M. 1995. *Properties of concrete*, fourth edition, Pearson, Prentice Hall, Essex, UK

Nowak, A.S. and Collins, K.R. 2013. *Reliability of structures* (2nd edition), CRC Press, Boca Raton, FL.

Perry, V.H. and Seibert, P.J. 2011. Working with Ductal ultra-high performance concrete, *Concrete Plant International*, 1(11), 2-5.

Resplendino, J. 2008. Ultra-high performance concretes—recent realizations and research programs on UHPFRC bridges in France, *Second International Symposium on Ultra High Performance Concrete*, Kassel, Germany, 31-43.

Rouse, J., Wipf, T.J., Phares, B.M., Fanous, F., and Berg, O. 2011. Design, construction, and field testing of an ultra-high performance concrete Pi-girder bridge, Bridge Engineering Center, Iowa State University, Ames, IA.0

Russell, H. and Graybeal, B. 2013. Ultra-high performance concrete: a state-of-the-art report for the bridge community, Report No. FHWA-HRT-13-060, Federal Highway Administration, Washington, D.C.

Semioli, W. 2001. The new concrete technology, *Concrete International*, 23(11), 75-79.

Strunge, J. and Deuse, T. 2008. Special cements for ultra-high performance concrete, *Second International Symposium on Ultra High Performance Concrete*, 61-68, Kassel, Germany.

Tafraoui, A., Escadeillas, G., Lebaili, S., and Vidal, T. 2009. Metakaolin in the formulation of UHPC, *Construction and Building Materials*, 23, 669-674.

Vanderberg, A. and Wille, K. 2018. Evaluation of resonance acoustic mixing technology using ultra high performance concrete, *Construction and Building Materials*, 164, 716-730.

Wille, K. Naaman, A. E., and Parra-Montesinos, G.J. 2011a. Ultra-high performance concrete with compressive strength exceeding 150 MPa (22 ksi): a simpler way, *ACI Materials Journal*, 108(1), 46-54.

Wille, K., Naaman, A.E., and El-Tawil, S. 2011b. Optimizing ultra-high performance fiber-reinforced concrete, *Concrete International*, 33(9), 35-41.

Yang, S.L., Millad, S.G., Soutsos, M.N., Barnett, S.J., and Le, T.T. 2009. Influence of aggregate and curing regime on the mechanical properties of ultra-high performance fibre reinforced concrete (UHPFRC), *Construction and Building Materials*, 23, 2291-2298.

Yoo, D.-Y., Lee, J.-H., and Yoon, Y.-S. 2013. Effect of fiber content on mechanical and fracture properties of ultra-high performance fiber reinforced cementitious composites, *Composite Structures*, 106, 742-753.

Zdeb, T. 2013. Ultra-high performance concrete: properties and technology, Bulletin of the Polish Academy of Sciences, 61(1), 183-193.

Appendix A: Test Data

Table A.1. Existing mixture design (Category I)

No.	Compressive strength at 28 days (ksi)			No.	Compressive strength at 28 days (ksi)		
	Each	Ave.	STDEV		Each	Ave.	STDEV
1 (AM)	16.8	17.00	2.16	6 (W)	16.2	13.43	2.48
	19.3				12.5		
	18.4				10.3		
	17.9				11.0		
	14.6				12.4		
	13.6				15.3		
	18.6				16.3		
2 (MO)	16.5	17.41	1.16	7 (WI)	13.8	15.51	1.62
	17.1				13.2		
	17.9				15.6		
	18.6				16.8		
	16.8				17.4		
	15.9				16.9		
	19.1				14.9		
3 (AH)	19.1	17.91	1.25	8 (AH)	17.6	21.23	2.33
	16.2				21.3		
	17.3				22.3		
	18.6				21.2		
	18.5				19.7		
	17.8				21.3		
	17.0				25.2		
4 (AS)	15.8	17.04	1.23	9 (AH)	20.4	22.50	1.92
	18.3				22.9		
	16.6				24.4		
	16.9				24.9		
	18.0				21.3		
	18.4				23.5		
	15.3				20.1		
5 (ZD)	16.4	17.41	1.70	AM = Al Madhoun (2013); M = Mohammed (2015); AH = Ahlborn et al. (2008b); AS = Askar et al. (2013); ZD = Zdeb (2013); W = Wille et al. (2011a); WI = Wille et al. (2011b)			
	18.9						
	15.7						
	16.6						
	16.4						
	17.4						
20.5							

Each = individual cylinder; Ave = average; STDEV = standard deviation

Table A.2. Finalized UHPC mixture design

Compressive strength (ksi)		
Each	Ave.	STDEV
20.6	20.26	0.56
20.4		
21.0		
19.8		
19.6		

Table A.3. Effect of silica fume types (Category III)

Type (days)	Compressive strength (ksi)			Type (days)	Compressive strength (ksi)		
	Each	Ave.	STDEV		Each	Ave.	STDEV
A (7)	13.8	12.94	1.89	C (7)	11.1	10.62	0.44
	15.6				10.6		
	10.9				9.9		
	11.4				10.8		
	13.0				10.7		
A (14)	14.3	15.72	1.74	C (14)	19.1	17.84	0.80
	18.5				17.3		
	15.6				17.9		
	16.0				17.0		
	14.2				17.9		
A (28)	19.8	17.12	1.88	C (28)	19.6	19.48	0.48
	17.9				19.1		
	17.2				20.2		
	15.1				19.5		
	15.6				19.0		
B (7)	11.9	11.96	0.71	D (7)	13.0	14.90	2.48
	10.9				13.3		
	12.7				13.1		
	11.8				16.8		
	12.5				18.3		
B (14)	15.9	16.16	0.58	D (14)	19.2	18.00	0.96
	16.5				17.3		
	15.8				17.0		
	17.0				18.8		
	15.6				17.7		
B (28)	19.5	18.3	0.72	D (28)	20.6	20.28	0.58
	18.3				20.4		
	18.1				21.0		
	17.6				19.8		
	18.0				19.6		

Table A.4. Effect of pyrogenic silica (Category IV)

Type (days)	Compressive strength (ksi)			Type (days)	Compressive strength (ksi)		
	Each	Ave.	STDEV		Each	Ave.	STDEV
VS-1 (7)	15.7	16.50	0.75	VS-3 (7)	16.7	16.38	0.55
	17.3				16.1		
	16.5				17.2		
	15.8				15.9		
	17.2				16.0		
VS-1 (14)	17.5	17.88	0.41	VS-3 (14)	17.5	17.52	0.31
	18.3				17.3		
	18.2				17.6		
	17.4				17.2		
	18.0				18.0		
VS-1 (28)	17.7	17.98	0.47	VS-3 (28)	18.7	18.40	0.78
	18.5				18.8		
	17.4				17.0		
	17.9				18.7		
	18.4				18.8		
VS-2 (7)	16.9	16.42	0.96	VS-4 (7)	16.2	16.22	0.38
	15.0				16.8		
	17.6				15.8		
	16.3				16.3		
	16.3				16.0		
VS-2 (14)	18.7	18.46	0.36	VS-4 (14)	15.4	16.52	0.89
	17.9				17.6		
	18.8				16.6		
	18.3				17.1		
	18.6				15.9		
VS-2 (28)	19.0	18.64	0.50	VS-4 (28)	19.0	18.40	0.47
	18.0				17.9		
	19.0				18.1		
	18.2				18.8		
	19.0				18.2		

Each = individual cylinder; Ave = average; STDEV = standard deviation

Table A.5. Effect of precipitated silica (Category IV)

Type (days)	Compressive strength, MPa (ksi)			Type (days)	Compressive strength, MPa (ksi)		
	Each	Ave.	STDEV		Each	Ave.	STDEV
VS-1 (7)	15.9	15.86	1.13	VS-3 (7)	15.6	15.56	0.46
	16.6				16.3		
	17.3				15.5		
	14.8				15.1		
	14.7				15.3		
VS-1 (14)	16.9	16.90	0.72	VS-3 (14)	18.0	17.94	0.57
	16.7				18.7		
	15.9				17.1		
	17.9				18.0		
	17.1				17.9		
VS-1 (28)	17.0	16.98	0.41	VS-3 (28)	17.9	17.98	0.95
	16.8				19.0		
	16.4				17.9		
	17.5				16.5		
	17.2				18.6		
VS-2 (7)	17.2	15.76	0.87	VS-4 (7)	16.9	15.52	0.94
	15.1				15.0		
	15.1				15.8		
	15.5				15.5		
	15.9				14.4		
VS-2 (14)	17.2	16.90	0.60	VS-4 (14)	17.8	17.76	0.77
	16.3				18.9		
	17.0				17.1		
	16.3				18.0		
	17.7				17.0		
VS-2 (28)	17.7	17.46	0.80	VS-4 (28)	18.2	18.14	0.53
	18.4				17.9		
	16.2				17.4		
	17.4				18.4		
	17.6				18.8		

Each = individual cylinder; Ave = average; STDEV = standard deviation

Table A.6. Effect of steel fibers (Category V)

Condition	Compressive strength (ksi)			Condition	Compressive strength (ksi)		
	Each	Ave.	STDEV		Each	Ave.	STDEV
With fibers	22.0	21.48	0.79	Without fibers	20.6	20.26	0.55
	20.3				20.4		
	22.3				20.9		
	21.1				19.8		
	21.7				19.6		

Each = individual cylinder; Ave = average; STDEV = standard deviation

Table A.7. Bond test data

Condition	Average bond stress (ksi)			Condition	Average bond stress (ksi)		
	Each	Ave.	STDEV		Each	Ave.	STDEV
With fibers	6.83	6.83	0.42	Without fibers	7.29	7.33	0.44
	7.37						
	6.34						
	6.82						

Each = individual cylinder; Ave = average; STDEV = standard deviation

Appendix B: State of the Art of UHPC

This appendix is excerpted from Kim (2013) and un-copied contents are provided.

Kim, Y.J. 2013. Recent advances in ultra-high performance concrete, Journal of Korean Recycled Construction Resources Institute 1(3), 163-172.

CHARACTERISTICS AND IMPLEMENTATION OF UHPC TECHNOLOGY

Design of UHPC

Typical concrete shows a compressive strength (f'_c) varying from 20 MPa to 35 MPa. The need for high strength and improved performance is emerging to build sustainable structures. The advent of reactive powder concrete with f'_c ranging from 200 MPa to 800 MPa overcomes the limitations of conventional normal strength concrete (Reactive 2002). UHPC addresses the following engineering characteristics: strength, elastic modulus, abrasion, durability, permeability, chemical resistance, impact, placement difficulty, and long-term maintenance costs. The strength range of UHPC exceeds the strength of high-strength concrete by two to six times (Lubbers 2003; Schneider et al. 2004). Table A1 compares typical engineering properties of UHPC with those of normal- and high-strength concrete. Although the theory of traditional reinforced concrete may be used for the application of UHPC, care should be exercised because numerous empirical factors were developed based on the behavior of conventional concrete. No codified provisions are available for UHPC in the United States. Therefore, experienced technical personnel can only assure the adequacy of UHPC design and construction. The optimal use of constituent materials is important for the implementation of UHPC. According to a comparative study (Blais and Couture 1999), steel fibers in UHPC (a length of 25 mm and a diameter of 0.2 mm) are equivalent to reinforcing bars of 8 mm in diameter and 1,000 mm in length for normal concrete. The removal of coarse aggregate reduces the interfacial transition zone between the cementitious binder and aggregates and thus improves tensile strength (Mindess et al. 2003; Mehta and Monteiro 2006). Supplementary cementitious materials such as silica fume fill micro-voids to produce a dense mixture with low permeability. Limited effort has been expended on using nano-scale materials for the design and practice of UHPC (Kowald 2004).

Table A1. Typical comparison of engineering properties of UHPC with normal and high strength concrete (compiled based on Ahlborn et al. 2008)

Property	Normal concrete	High strength concrete	UHPC
Compressive strength	3,000-6,000 psi	6,000-14,000 psi	25,000-33,000 psi
Tensile strength	400-500 psi	-	1,000-3,500 psi
Elastic modulus	2,000-6,000 ksi	4,500-8,000 ksi	8,000-9,000 ksi
Poisson's ratio	0.11-0.21	-	0.19-0.24
Porosity	20-25%	10-15%	2-6%
Chloride penetration	>2000	500-2000	<100
Water-cement ratio	0.40-0.70	0.24-0.35	0.14-0.27

Material composition

Most composition of UHPC is dry particles, while liquid-oriented constituents are limited. UHPC is typically composed of portland cement, supplementary cementitious materials, quartz powder, water, fine aggregate, a superplasticizer, and fibers. The use of fine aggregate and quartz powder increases density, whereas it decreases porosity. The particle size of fine aggregate affects the homogeneity of UHPC (Richard and Cheyrezy 1995). Quartz is easily obtainable and possesses a very high compressive strength (1,100 MPa) at an inexpensive price (about \$150 per ton). Steel or organic fibers are commonly used for UHPC, including a fiber ratio from 1.0% to 2.0% (Al-Azzawi et al. 2011). Because of the embedded fibers, the crack width of UHPC is much smaller than that of conventional concrete (FHWA 2011). The effect of fiber content influences the post-peak behavior of UHPC in tension, while such an effect may not be critical for compressive strength (Ali 2007; Redaelli and Muttoni 2007; Al-Azzawi et al. 2011). Attention needs to be paid when the tensile strength of UHPC is measured because the internal fibers can have an impact on the cracking response of the concrete such as strain-hardening (FHWA 2011). Silica fume and high reactivity metakaolin are widely used materials (Ali 2007). Silica fume includes amorphous silica dioxide and reacts with calcium hydroxide (Al-Azzawi et al. 2011). Metakaolin is white clay and is obtained by treating kaolin. Metakaolin (typically 0.005 mm in diameter) is an abundant material and its primary composition includes SiO₂ and Al₂O₃ (Sabir et al. 2001). These supplementary cementitious materials chemically react during the hydration process of cement, so that the performance of UHPC is enhanced. A compressive strength of 97 MPa may be a good indicator of adequate hydration (FHWA 2011). Qian and Li (2001) reported that the tensile strength and corresponding strain of concrete increased with an

increasing metakaolin content, whereas the elastic modulus of the concrete was independent of metakaolin. UHPC mixed with silica fume showed a higher compressive strength than that with high reactivity metakaolin (Al-Azzawi et al. 2011). Due to the dense mixture of the constituents, UHPC demonstrates a low permeability (Ahlborn et al. 2008). The performance of UHPC is enhanced accordingly, such as freeze-thaw resistance and reduced corrosion of reinforcing steel. The permeability of concrete controls chloride penetration, thereby increasing the corrosion potential of embedded reinforcing steel bars (Lubbers 2003; Ahlborn et al. 2008). UHPC effectively addresses this concern according to experimental investigations (e.g., oxygen permeability less than 3.9×10^{-12} mm², AFGC 2002). The water-cementitious binder ratio of UHPC (typically ≤ 0.25) is lower than that of normal concrete. A superplasticizer improves workability that may be problematic because of such a low water-binder ratio. Collepardi et al. (1996) studied the efficacy of a superplasticizer and silica fume on the compressive strength of UHPC. Test results include that acrylic polymer demonstrated better performance than sulfonated melamine and sulfonated naphthalene. Strength gain at the early age of UHPC is of interest. The reason is that UHPC exhibits a gradual decrease in strength with time owing to a reduction in water content and the chemical reaction associated with supplementary cementitious materials commencing in a few days of concrete-casting (Al-Azzawi et al. 2011). Although research has been conducted as to the behavior of UHPC with carbon nanotubes, it is still inconclusive (Wille and Loh 2010). For example, an increase in compressive strength over 12% was observed when multi-walled carbon nano tubes (MWNT) were included in a UHPC mixture (Li et al. 2005; Kowald et al. 2008); however, some experimental programs reported that the inclusion of MWNT caused a reduction in strength (Musso et al. 2009). Alternative nano-scale materials may be used for the formulation of UHPC, such as nano silica.

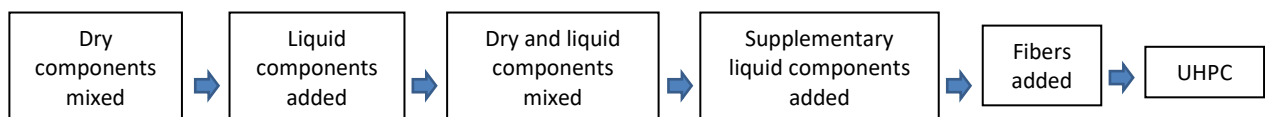


Fig. A1. Typical sequence of mixing UHPC

Mixing, curing, and formulation procedures

Mixing is an important component to attain the best performance of UHPC. Figure A1 shows typical procedures to mix UHPC. The mixture design and procedures of UHPC differ from those of normal concrete. Selected mix designs for UHPC are summarized in Table A2. Improving the density of UHPC is a critical factor to accomplish high strength and durable performance when subjected to aggressive service conditions. The particle size of aggregate needs to be carefully determined because it controls the homogeneity of UHPC. Improved homogeneity increases the reliability of UHPC (Lubbers 2003). UHPC uses significantly smaller aggregates in comparison with other types of concrete (Richard and Cheyrezy 1995; Bonneau et al. 1997): cement particles (0.01 mm to 0.08 mm), quartz powder (0.01 mm to 0.015 mm), and silica fume (0.1×10^{-6} mm to 0.2×10^{-6} mm). Typical size of steel fibers in UHPC is 0.2 mm in diameter and less than 25 mm in length (Blais and Couture 1999). Embedded fibers tended to align in the direction of concrete flow when UHPC is cast and thus the modification of concrete rheology requires technical attention (FHWA 2011).

Table A2. Composition of materials for UHPC (percent by weight)

Reference	Cement	W/C ratio	Fiber	SCM	Quartz powder	Super-plasticizer	Sand	Compressive strength
B&C	28%	0.28	7%(S)	9%(SF)	8%	1%	40%	200 MPa
Bonneau	28%	0.27	6%(S)	9%(SF)	9%	2%	41%	190 MPa
HDR	37%	0.14	6%(S)	9%(SF)	0%	2%	41%	160 MPa
R&C	32%	0.19	6%(S)	7%(SF)	13%	1%	35%	200 MPa
W&L	32%	0.22	0.007%(CNT)	8%(SF)	8%	0.2%	44%	194 MPa
Ahlborn	26%	0.20	6%(S)	Pre	Pre	1%	Pre	194 MPa

W/C ratio = water cement ratio; S = steel fiber; O = organic fiber; CNT = carbon nanotube; SF = silica fume; Pre = premix; SCM = supplementary cementitious material; HDR = HDR Inc (2002); R&C = Richard and Cheyrezy (1995); Bonneau = Bonneau et al. (1997); B&C = Blais and Couture (1999); W&L = Wille and Loh (2010); Ahlborn = Ahlborn et al. (2008)

The embedded fibers can replace temperature and shrinkage steel reinforcement in concrete. In some cases, shear stirrups are not included in a reinforced concrete beam (Reactive 2002). Supplementary cementitious materials can fill the pore space between constituents so that the durability performance of UHPC is improved (Lubbers 2003). To maintain the water-cementitious binder ratio of an UHPC mixture as designed, the surface of the concrete should be covered immediately after a casting event. It is important to note that water content affects the behavior of UHPC because the concrete requires a hydration process. Inadequate hydration

action causes premature shrinkage cracks and degraded engineering properties (FHWA 2011). The low water-cementitious binder ratio of UHPC may cause disintegration of the constituents during mixing. The inclusion of nano particles may improve the bond between the steel fibers and cementitious binder of UHPC (Wille and Loh 2010). Special procedures are required to ensure consistent quality on site. Care should be exercised when casting UHPC because of its extended setting time and potential segregation (i.e., discrete fibers may not function well if excessive vibration is applied). The mixing procedures of UHPC can thus influence material properties depending upon the sequence and mixing time (Lubbers 2003).

Supplementary treatment

A variety of treatment methods are used to enhance the performance of UHPC. Heat treatment during the curing of UHPC can accelerate the action of silica fume, resulting in an increase in strength (Schachinger et al. 2008). Previous research reports that optional heat treatment has improved the strength of UHPC as high as 70% (Bonneau et al. 1997). Typical conditions for such heat treatment include a temperature range between 50°C and 90°C in moisture for 48 hours (Bonneau et al. 1997; Reda et al. 1998). Heat treatment can reduce shrinkage and creep by improving the reaction of silica fume and a hydration process (Bouygues et al. 2002). It should, however, be noted that overheating may take place when UHPC is mixed because of its longer mixing time compared with conventional concrete (FHWA 2011). Improvement in mix-procedures is necessary to preclude potential heat-induced residual damage in UHPC. Ahlborn et al. (2008) examined the effects of steam treatment on the strength variation of UHPC, including durability performance. Test results showed that UHPC effectively resisted freeze-thaw and chloride ion penetration. Additional pressure may be applied to reduce the porosity of UHPC that is caused by the LeChatelier contraction (Aitcin 1998). The pressure applied during curing tends to decrease porosity by reducing entrapped air and excessive water; consequently, the compressive strength of the concrete increases (Blais and Couture 1999).

Test methods

Standard test methods are currently unavailable for measuring the properties of UHPC. The following test methods developed for concrete materials may be used for UHPC until specific standards are published. ASTM C39 (*Standard test method for compressive strength of*

cylindrical concrete specimens) and C109 (*Standard test method for compressive strength of hydraulic cement mortars*) can be used for the compressive test of UHPC (ASTM 2011, 2012a). ASTM C469 (*Standard test method for static modulus of elasticity and Poisson's ratio of concrete in compression*) may be used to measure the elastic modulus of UHPC (ASTM 2010a). ASTM C1018 (*Standard test method for flexural toughness and first-crack strength of fiber-reinforced concrete*) will be a reference for examining the flexural strength of UHPC (ASTM 1997). ASTM C1437 (*Standard test method for flow of hydraulic cement mortar*) can measure the rheological characteristics of UHPC (ASTM 2007). ASTM C1202 (*Standard test method for electrical indication of concrete's ability to resist chloride ion penetration*) may be used to assess the degree of chloride penetration (ASTM 2012b). AASHTO TP-60-00 (*Standard method of test for coefficient of thermal expansion of hydraulic cement concrete*) may be utilized to measure the coefficient of thermal expansion (AASHTO 2007). If the long-term behavior of UHPC is of concern, ASTM C512 (*Standard test method for creep of concrete in compression*) will be useful for a creep test (ASTM 2010b). The freeze-thaw durability of the concrete may be examined by ASTM C666 (*Standard test method for resistance of concrete to rapid freezing and thawing*) (ASTM 2008b).

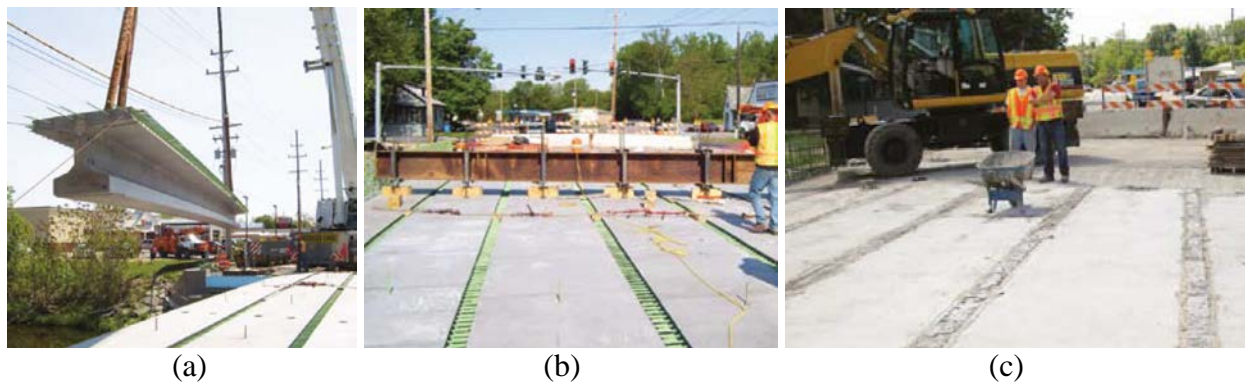


Fig. A2. UHPC joint (photos are used with permission from ASPIRE): (a) erection of a bulb-tee girder; (b) installed steel cage for a UHPC joint; (c) casting of UHPC

Site implementation

Potential application of UHPC is broad such as bridge structures, tunnels, nuclear power plants, and liquid storage facilities. UHPC is an ideal material for structures exposed to an abrasion environment. Several site projects using UHPC have been completed, including Sherbrooke

Footbridge in Canada, Footbridge of Peace in Korea, and Jakway Park Bridge in the United States (Blais and Couture 1999; Resplendino and Petitjean 2003; Kollmorgen 2004; Schmidt and Fehling 2005; Rouse et al. 2011; Planete 2012). Figure A2 illustrates selected examples on UHPC-based bridges in the United States: the depth and length of the girders shown in Fig. A2 (a) and (b) vary from 838 mm to 1,143 mm and 25.9 m to 26.5 m, respectively. Another application is given in Fig. A3 with the details of UHPC joints connecting bulb-tee girders. A comprehensive study of UHPC was recently published by the Federal Highway Administration (Graybeal 2006). Steel fibers are widely used for site application, while polypropylene fibers can improve permeability as well as abrasion and impact resistance (Toutanji 1999; Lubbers 2003). Considering the reduced use of reinforcing steel, more versatile architectural and structural design may be available. The increased toughness of UHPC makes this material ideal for concrete structures in seismic regions (Reactive 2002). Although the initial expenses associated with UHPC are more than those of normal concrete, material costs are consistently decreasing with more site projects.



(a)



(b)



(c)

Fig. A3. Bridges with UHPC (photos are used with permission from ASPIRE): (a) Cat Point Creek Bridge in Warsaw, Virginia; (b) Jakway Park Bridge, Aurora, Iowa; (c) State Route 23 over Otego Creek, Oneonta, New York

REFERENCES

AASHTO. 2007. Standard method of test for coefficient of thermal expansion of hydraulic cement concrete (AASHTO TP-60-00), American Association of State Highway and Transportation Officials, Washington, D.C.

AFGC. 2002. Ultra high performance fibre reinforced concretes, Interim Recommendations, Association Francaise de Genie Civil, France.

Ahlborn, T.M., Peuse, E.J., and Misson, D.L. 2008. Ultra-high performance concrete for Michigan bridges, Center for Structural Durability, Michigan Technological University, Houghton, MI.

Aitcin, P. 1998. High-performance concrete, Routledge, NY.

Al-Azzawi, A., Ali, A.S., and Risan, H.K. 2011. Behavior of ultra-high performance concrete structures, ARPN Journal of Engineering and Applied Sciences, 6(5), 95-109.

Ali, A.S. 2007. Mechanical properties and durability of polymer modified RPC exposed to oil products, PhD Thesis, University of Technology, Bagdad, Iraq.

ASTM. 1997. Standard test method for flexural toughness and first-cracking strength of fiber-reinforced concrete using beam with third-point loading (ASTM C1018-97), American Society for Testing and Materials, Conshohocken, PA.

ASTM. 2007. Standard test method for flow of hydraulic cement mortar (ASTM C1437-07), American Society for Testing and Materials, Conshohocken, PA.

ASTM. 2008b. Standard test method for resistance of concrete to rapid freezing and thawing (ASTM C666-08), American Society for Testing and Materials, Conshohocken, PA.

ASTM. 2010a. Standard test method for static modulus of elasticity and Poisson's ratio of concrete in compression (ASTM C469-10), American Society for Testing and Materials, Conshohocken, PA.

ASTM. 2010b. Standard test method for creep of concrete in compression (ASTM C512-10), American Society for Testing and Materials, Conshohocken, PA.

ASTM. 2011. Standard test method for compressive strength of hydraulic cement mortars (ASTM C109-11), American Society for Testing and Materials, Conshohocken, PA.

ASTM. 2012a. Standard test method for compressive strength of cylindrical concrete specimens (ASTM C39-12), American Society for Testing and Materials, Conshohocken, PA.

ASTM. 2012b. Standard test method for electrical indication of concrete's ability to resist chloride ion penetration (ASTM C1202-12), American Society for Testing and Materials, Conshohocken, PA.

Bonneau, O., Lachemi, M., Dallaire, E., Dugat, J., and Aitcin, P. 1997. Mechanical properties and durability of two industrial reactive powder concretes, *ACI Materials Journal*, 94(4), 286-290.

Bouygues, Lafarge, and Rhodia. 2002. Ductal. www.ductal.com

Blais, P. and Couture, M. 1999. Precast, prestressed pedestrian bridge- world's first reactive powder concrete structure, *PCI Journal*, 44(5), 60-71.

Colleparidi, S., Coppola, L., Troli, R., and Colleparidi, M. 1996. Mechanical properties of modified reactive powder concrete, *International Conference on Superplasticizers and the Chemical Admixtures in Concrete*, ACI-SP173, 1-21.

FHWA. 2011. Tech note: ultra-high performance concrete, FHWA-HRT-11-038, Federal Highway Administration, Washington, D.C.

HDR. 2002. Tensile properties of VHSC, HDR, Inc. (adopted from Lubbers 2003)

Graybeal, B.A. 2006. Material property characterization of ultra-high performance concrete, FHWA-HRT-06-103, Federal Highway Administration, Washington, D.C.

Graybeal, B.A. 2009. UHPC making strides, Public Roads, Federal Highway Administration, Washington, D.C., 72(4), 17-21.

Kollmorgen, G.A. 2004. Impact of age and size on the mechanical behavior of ultra-high performance concrete, MS Thesis, Michigan Technological University, Houghton, MI.

Kowald, T. 2004. Influence of surface modified carbon nanotubes on ultra-high performance concrete, Proceedings of the International Symposium on Ultra High Performance Concrete, Kassel, Germany, 195-202.

Kowald, T.R., Trettin, N., Dorbaum, T., Stadler, T., and Jian, X. 2008. Influence of carbon nanotubes on the micromechanical properties of a model system for ultra-high performance concrete, Proceedings of 2nd International Symposium on Ultra High Performance Concrete, 129-134.

Li, G.Y., Wang, P.M., and Zhao, X. 2005. Mechanical behavior and microstructure of cement composites incorporating surface-treated multi-walled carbon nanotubes, Carbon, 43(6), 1239-1245.

Lubbers, A.R. 2003. Bond performance between ultra-high performance concrete and prestressing strands, MS Thesis, Ohio University.

Mehta, P.K. and Monteiro, P.J.M. 2006. Concrete microstructure, properties, and materials, McGraw-Hill, New York, NY.

Mindess, D., Young, J.F., and Darwin, D. 2003. Concrete: 2nd edition, Pearson Education, Upper Saddle River, NJ

Musso, S., Tulliani, J.M., Ferro, G., and Tagliaferro, A. 2009. Influence of carbon nanotubes structure on the mechanical behavior of cement composites, *Composites Science and Technology*, 69(11-12), 1985-1990.

Planete TP. 2012. The world of public works, www.planete-tp.com/en

Qian, X. and Li, Z. 2001. The relationships between stress and strain for high-performance concrete with metakaolin, *Cement and Concrete Research*, 31, 1607-1611.

Reactive powder concrete. 2002. Emerging Construction Technologies, www.new-technologies.org/ECT/Civil/reactive.htm

Reda, M., Shrive, N., and Gillot, J. 1998. Microstructural investigation of innovative UHPC, *Cement and Concrete Research*, 29(3), 323-329.

Redaelli, D. and Muttoni, A. 2007. Tensile behavior of reinforced ultra-high performance fiber reinforced concrete elements, *Concrete Structures- Stimulators of Development*, 267-274.

Resplendino, J. and Petitjean, J. 2003. Ultra-high performance concrete: first recommendations and examples of application, 3rd International Symposium on High Performance Concrete, PCI, Orlando, FL.

Richard, P. and Cheyrezy, M. 1995. Composition of reactive powder concretes, *Cement and Concrete Research*, 25(7), 1501-1511.

Rouse, J., Wipf, T.J., Phares, B.M., Fanous, F., and Berg, O. 2011. Design, construction, and field testing of an ultra-high performance concrete Pi-girder bridge, Bridge Engineering Center, Iowa State University, Ames, IA.

Sabir, B.B., Wild, S., and Bai, J. 2001. Metakaolin and calcined clays as pozzolans for concrete: a review, *Cement and Concrete Composites*, 23, 441-454.

Schachinger, I., Hilbig, H., and Stegel, T. 2008. Effect of curing temperature at an early age on long-term strength development of UHPC, 2nd International Symposium on Ultra High Performance Concrete, Kasel, 205-212.

Schmidt, M. and Fehling, E. 2005. Ultra-high performance concrete: research, development, and application in Europe, 7th International Symposium on the Utilization of High-strength/High-performance Concrete, ACI-SP-228, 51-78.

Schneider, H., Smisch, G., and Schmidt, D. 2004. Bearing capacity of stub columns made of NSC, HSC, and UHPC confined by a steel tube, *Cement and Concrete Research*, University of Leipzig, 122-130.

Semioli, W. 2001. The new concrete technology, *Concrete International*, 23(11), 75-79.

Toutanji, H. 1999. Properties of polypropylene fiber reinforced silica fume expansive cement concrete, *Construction and Building Materials*, 13, 171-177.

Willie, K. and Loh, K.J. 2010. Nanoengineering ultra-high-performance concrete with multiwalled carbon nanotubes, *Journal of Transportation Research Board*, No. 2142. 119-126.